Project acronym: AMEDEUS
Project full title: Accelerate Membrane Development for Urban Sewage Purification
Proposal/Contract no.:018328 AMEDEUS
Duration: Oct. 2005 – Sept. 2008

WP1 - TEXTILE MATERIAL FOR MBR FILTRATION
D1 – Characterisation tests on selected nonwoven webs (at least six webs made of three fibres)
D7 – WP1 Report

Authors

Enrico Fatarella	TTX
Vera Iversen	TUB
Stefan Grinwis	A3
Sabine Paulussen	VITO

Report delivery date
May 2009

Quality Management

	Name	Company	Date
Final edition	Enrico Fatarella	TTX	10 June 2009
1st control	Steffen Richter	A3	4 June September 2009
2nd control	Vera Iversen	TUB	10 May 2009
3rd control	Sabine Paulussen	VITO	21 September 2007

Project co-funded by the European Commission within the Sixth Framework Programme (2002-2006)

Dissemination Level

PU	Public	**X**
PP	Restricted to other programme participants (including the Commission Services)	
RE	Restricted to a group specified by the consortium (including the Commission Services)	
CO	Confidential, only for members of the consortium (including the Commission Services)	

Revision: Final version

SIXTH FRAMEWORK PROGRAMME
Priority 1.1.6.3
"GLOBAL CHANGE AND ECOSYSTEMS"

SPECIFIC TARGETED RESEARCH PROJECT

Index:

1 Introduction

Membranes used in MBR process are generally microfiltration membrane (MF) or ultrafiltration membrane (UF). The membrane materials commercially used in MBR process include ceramics and both unmodified and surface modified polymeric materials, such as polyethylene, polypropylene and polysulfone[i]. The pore sizes of these membrane materials are usually in the 0.02μm~0.5μm range. Therefor bacteria, colloids, inorganic ion and smaller size organic micropollutants, such as humic acid in water treatment are removed by the membrane. In activated sludge system, it also includes the sludge flocs whose size range from 1μm to hundreds of μm, and colloidal and soluble fractions. Textile filtration media may be an economical option compared with polymeric micro- or ultrafiltration membranes, due to the lower cost per unit of surface and the potentially greater filtration flux[ii]. especially for applications were the high hygienic standard of an MBR is not necessary.
It is well known that non-woven fabric materials are extensively used for the removal of particles larger than 1μm in decontamination process, especially in air filtration[iii] and lately they have been applied as a filter material for domestic wastewater treatment coupled with activated sludge system[iv]. Non-woven fabric materials are composed of random network of overlapping fibers. They can create multiply connected pores through which the fluid can flow. Non-woven fabric filtration material has many outstanding properties, such as controllable pore size distribution and easy design of fiber surface area per unit weight and volume. For comparing also woven textiles have been tested, though they are commonly dearer due to the more complex production process. In literature wovens[vvi] as well as non wovens[viiviii] have been tested for the application in bioreactors but the research is at an early stage and so far non woven materials have not found commercial application for MBR.
The aim of this study was to characterise textile membranes available in the market (10 membranes) and newly realised by TTX (8 membranes). Polypropylene and Nylon 6,6 (Polyamide) were used as raw materials, since they were most suitable one in term of costs and treatability with Melt-Blown technology.
The characterisation is required to investigate the adaptability of the textile membranes in the MBR process in term of mechanical and chemical properties and in term of filtration efficiency in comparison with a conventional membrane provided by A3 and also to verify the possibility to implement the textile material in the A3 production line.
In the same time deposition of nanoweb on the surface of non woven membranes and plasma treatments are investigating to improve the performance and to ensure an easy application in the MBR processes of selected membranes.

2 Materials and Methods

2.1 Membrane Characterisation

10 commercial membranes and 8 newly realised membranes were characterised within WP1 (Table 1).

Table 1 – List of textile membranes studied within the WP1

Sample ID
A3 membrane
PA_5mm*
PA_10mm*
PA_15mm*
PA_24mm*
PP_10mm*
PP_15mm*
PP_24mm*
PP_50mm*
POLYNOVA
SFT_10mm
SFT_1mm
SEFAR
Chaussette
2325990502 or 10 micron
16P05A Solupor
E-9H01A Solupor
E-9H06A Solupor
Viledon

* Membrane sample produced at TTX

Textile membranes were characterised by means of:

- *FT-IR analyses* to confirm the chemical composition of the commercial membranes.
  The infrared (IR) spectra of studied samples were recorded by means of a Perkin Elmer Spectrum One spectrometer in HATR reflection mode using a zinc selenide crystal. An average of 16 scans using a resolution of 4 cm^{-1} was used.
- *Thermal Gravimetric Analysis* (TGA) to investigate the wettability, as wet pick-up, of the polymeric material used to produce the studied membranes and to define thermal degradation behaviour of each materials. Thermalgravimetric analyses were carried out by means of a Mettler Toledo TGA – STDA 851^e equipment. Pierced aluminium pans were used as sample holders and an empty pan was used as reference. Approximately 7-10 mg of the sample was used per measurement, it was placed into the pan and weighed. The pans were closed and two holes were pierced into the lid of each pan just before placing it into the TGA machine. The study was carried out over a temperature range of 25-600°C. We have used heating rates of 10 K/min and a nitrogen flow of 60 mL/min for washing the cells.
- *Chemical Resistance to acid (HNO_3, 1 M at pH < 2); to alkali (NaOH, 1 M at pH > 12); to chloride (NaOCl, 1000 ppm) and to hydrogen peroxide (H_2O_2, 500 ppm)*[ixx].
  Tests were carried out on 10 x 5 cm^2 samples in the previous solutions for 16 hours at a temperature of 60 °C in agreement with an internal method extracted from the Standard Test ISO 1817 “Rubber, vulcanised - Determination of the effects of liquid”.
  The resistance of the membranes were evaluated by means of:
  - Gravimetric analyses: the membranes, conditionated for 24 h at 20 °C and at relative humidity of 65%, were weighted before and after each treatment.
  - Tensile strength and elongation measurement before and after the treatment by means of Standard Test (ASTM D638).

- Thermal Analysis by means of Differential Scanning Calorimetry (DSC) to investigate if the treatment could affect the arrangement of the polymer chains in terms of crystallinity. The thermal measurements were carried out on a Mettler STAR DSC. Pierced aluminium pans were used as sample holders and an empty pan was used as reference. Approximately 7-10 mg of the sample was used per measurement. Prior to measurement all the samples were cut into small snippets, conditioned for at least 24 hours in a climatic room at 65% RH and 20°C, and then placed into the aluminium pan and weighed. The pans were closed and two holes were pierced into the lid of each pan just before placing it into the DSC machine. The study was carried out over a temperature range of 25-450°C. We have used heating rates of 10 K/min and a nitrogen flow of 80 mL/min for washing the cells. Each experiment has been resumed three times, and the data given below are their mean values.

- *Roughness measurements* assessed, using a scanning topography measurements instrument (Altisurf 500). The device is based on the principle of chromatic aberration, the capacity of the gauge lens to focus different colors in different focal planes. The focusing wavelength (reflected by the sample) is analysed by the probe spectrophotometer, which analyses the distance of the lens at the surface.

- *Pore size analysis by means of Capillary flow porometry* to verify the real pore size for the commercial and newly realised membranes.
  A liquid, whose surface free energy with the sample is lower than that of the sample with gas is used to fill the pores of the sample. Because of the reduction in the free energy of the system the pores are filled spontaneously. A non-reacting gas is employed to force the liquid out of the pores. The gas can displace the liquid in a pore, provided work done by gas is equal to the increase in surface free energy required for the replacement of the low free energy sample-liquid surface by the high free energy sample –gas surface (Figure 1)[1].

  $p\ dV = (\gamma s/g - \gamma\ s/l)\ dS$ (1)

  where p is differential pressure, dV is displaced volume of liquid in the pore, γs/g is solid-gas surface free energy, γs/l is solid-liquid surface free energy and dS is increase in solid-gas surface area (decrease in solid-liquid surface area). The change in the liquid-gas inter-facial area is usually negligible [2].

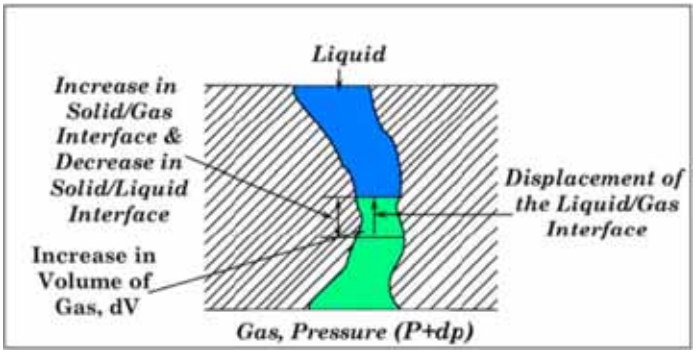

Figure 1 - Displacement of wetting liquid in a pore.

Consideration of equilibrium between surface tensions (Figure 2) leads to [3]:

$(\gamma s/g - \gamma\ s/l) = \gamma \cos \theta$ (2)

where γ is the surface tension and θ is the contact angle of the wetting liquid. From Equations 1 and 2:

$p = \gamma \cos \theta\ (dS/dV)$ (3)

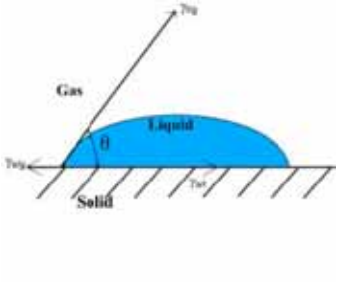

Figure 2 - Equilibrium between surface tensions.

Definition of pore diameter: Pore surfaces normally converge and diverge in irregular manner creating irregular pore cross-sections along pore path. Consequently, a pore cross-section may not be associated with a well defined pore diameter. A few examples are illustrated in Figure 3.

Figure 3 - Pore cross-sections.

The pore diameter, D, is defined such that:

(dS/dV)pore = (dS/dV)circular opening of diameter, D = 4/ D (4)

From Equations 3 and 4:

p = 4 γ cos θ / D (5)

Equation 5 suggests that increasing gas pressure removes liquid from decreasing pore diameter. The liquid extrusion techniques measure differential gas pressure, gas flow rates through emptied pores or volume of extruded liquid. Many pore structure characteristics are computed from these measured quantities. Capillary flow porometry is a liquid extrusion technique in which the differential gas pressure and flow rates through wet and dry samples are measured (Figure 4) [4]. Pore diameters, the largest pore diameter, the mean flow pore diameter, pore distribution; envelope surface area (through pore surface area) and gas permeability are computed. Liquid permeability is also measurable in this technique.

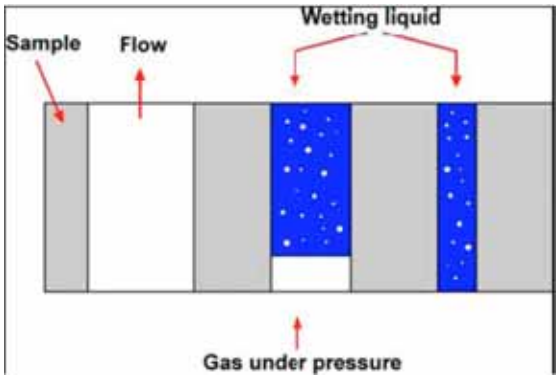

Figure 4 - Principle of capillary flow porometry.

The Capillary Flow Porometer (Porus Materials, Inv. Analytical Services Division) has capability for fully automated test execution, data acquisition, data storage and data reduction.
The windows based operation of the instrument is simple. The output of the instrument is reproducible and accurate.

- *Tests with a cross-flow-filtration test cell (TUB)* Filtration tests were done with two different sludges: 1) Sludge from a small scale MBR operated with synthetic wastewater under constant conditions at the department for Chemical Engineering 2) Sludge from the containerized

AMEDEUS pilots operated with municipal wastewater near a pumping station of the local water supplier (Berliner Wasserbetriebe). The sludge properties for 1) were assumed to be similar in terms of filtration on different days while sludge from 2) can change due to different influent and temperature conditions . Filtration tests were carried out in a cross-flow filtration test cell designed at the department[xi], representing the conditions between two flat sheets in a submerged plate and frame module, Figure 5. Several measuremant series were conducted:

- TMP = const. Tests were carried out under constant pressure conditions of approx. 0.6-0.65 bar. Cross-flow velocity was constant at 0.2 m/s. A slightly higher TMP than during normal flat sheet operation had to be chosen to enable comparison of all textiles at the same conditions, i.e. to obtain a measurable flux even for very dense nonwovens. Flux decline was measured until constant flux was achieved. All tests were conducted with sludge from 1).

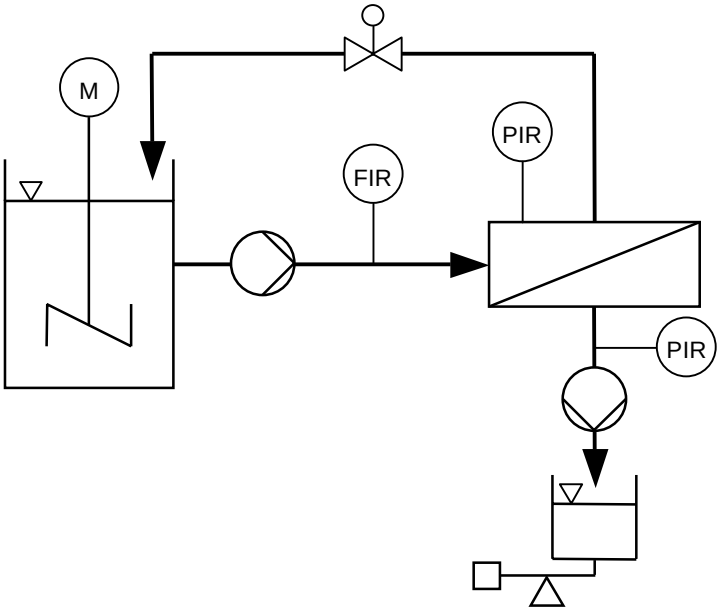

Figure 5– Flow-sheet of the cross flow membrane test cell

- Critical flux. The critical flux was determined according to Figure 6 with the flux-step method. The test-cell was aerated in a vertical setup. For the determination of the critical flux all data was plotted on same scale and the first flux for which a significant increase of TMP during one flux step occurred was defined the critical flux (a critical flux of 215LMH was defined for Figure 6).

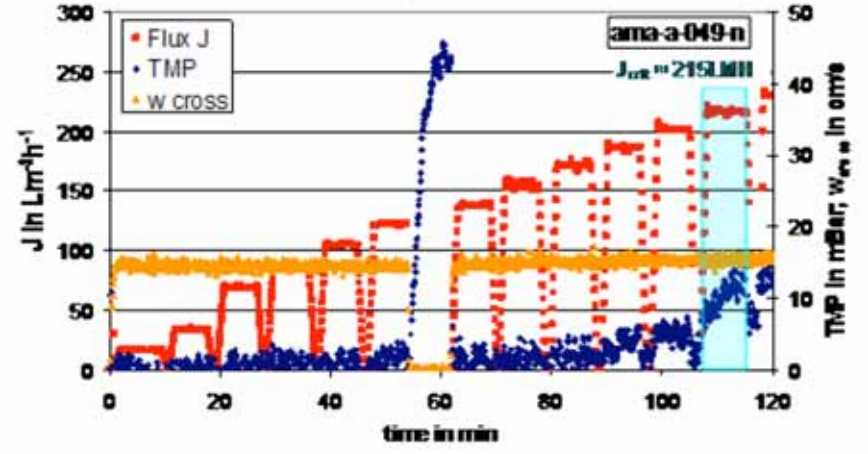

Figure 6 – Determination of the critical flux

- Parameter optimization The optimization of filtration was conducted with different filtration strategies (wash on of filter cake), different parameters for the crossflow velocity, the aeration and the flux. Also the different sludges and the addition of flocculant were tested.

Long Term filtration tests

From their short-term performance the following textile have been selected for long term testing. Membrane used by A3 (Microdyn-Nadir, PVDF, 0.2µm) was used as a reference (Table 2).

Table 2 –Non woven membrane characterised at TUB

Sample ID	Commercial name
A4	FF2007
D1	SFT 1 μm
G2	TTX, PP 10 μm
G3	TTX, PA 10 μm
H1	E9H01A
H4	16P05A
Control	A3, PVDF, 0.2 μm

Tests were conducted over 10-12h in the filtration test cell shown in Figure 5. In order to have a better simulation of operation conditions, the test cell was vertically operated under constant flux conditions (15-16L m-2 h-1) with 10min pulse and 2min pause. It was aerated with an air flow rate of 77L/h. TMP was recorded over time, if the fouling was to severe the experiment was stopped. Prior to the experiment the test cell,pipes and equipment were disinfected by heat or ethanol. The filtration media was evaluated in terms of fouling and of retention of chemical oxygen demand (COD), polysaccharides, proteins and permeate quality at the end of each experiment.

The following procedures were used:

- COD: Sludge was centrifuged for 20min at 10000g. Samples of the permeate were analyzed without pre-treatment. COD was analyzed with a commercial test (Hach Lange GmbH, LCK 514 for sludge supernatant and very turbid permeates, LCK 314 for permeates)
- Proteins and Polysaccharides: Permeate and sludge samples were centrifuged for 20min at 10000g. Polysaccharide concentrations were determined according to Dubois et al.[xii], calibration was done with D-glucose-monohydrate in a range between 2-100mg/L. Protein concentrations were determined according to Frolund et al.[xiii] with a calibration range of 2-200mg/L bovine serum albumin (photometer: Specord 200, Carl Zeiss).
- Turbidity: Extinction of permeate samples were measured photometrically for wavelengths of 860nm and 520nm (photometer: Specord 200, Carl Zeiss) Also turbidity units FAU were measured in accordance with DIN EN ISO 7027.
- Hygienic quality: Permeate samples were taken with a sterile syringe and diluted by the factor 10^{-3} and 10^{-7}. 100µl diluted sample were brought on a agar plate. LB Luria-Bertani (tryptone, yeast extract and natriumchlorid were dosed factor 10 lower) or DEV (Merck KGaA, Darmstadt, Germany) media was used for cultivation.

Adequacy of the non woven membrane materials in MBR module

Commercial 25 μm polypropylene and polyaminde membranes were provided to A3 by TTX in order to verify the adaptability of the non woven membrane materials to the module production process and to judge its from a manufacturers point of view. The following tests were performed:

- Strength: The membrane material was treated mechanically on one hand at the manufacturing machine to simulate the mechanical stress that occurs during the production process, by clamping it onto the feed roll, and on the other hand visually and by “self-treatment”, to evaluate the adequacy of material when operating an MBR.
- Desorption of water and organic solvent, stability to organic solvent: the materials were weighted dry and stored in water and as well in acetone (main solvent within the potting process) for 1h – 1day – 1 week at 20°C to test the liquid adsorption of the pores, as well as the stability of the material. To simulate the conditions in an MBR, the material was dried several times up to weight constancy.

- Cushion-production on a small scale by varying and evaluating the optimum of temperature and time for laminating: For this test, the production machine needs to be fitted with small manufacturing frames, because of the small scale of delivered sheets, in normal cases, the material is rolled. Several cushions were produced manually by welding the side by varying the important factors time and temperature. Within the same tests, it becomes visible, if the production machine can handle the material in the automatic process or if there is any inadequacy.
- Potting test: the second important interconnection in the production process is a potting between the membrane cushion and a glue that hards out. For this test, both available materials were combined with the standard potting procedure of A3 and afterwards with a variation of hardening time and temperature to minimize the effects of an occurring desorption of organic solvent.

2.2 Electrospun nanofibers for filtration applications

Electrospinning process allows to produce nanofibers from different polymer. This technique permits to produce polymer filaments using electrostatic force. In the electrospinning process a high voltage is used to create an electrically charged jet of polymer solution or melt, which dries or solidifies to leave a polymer fiber. One electrode is placed into the spinning solution/melt and the other attached to a collector. Electric field is subjected to the end of a capillary tube that contains the polymer fluid held by its surface tension. This induces a charge on the surface of the liquid. Mutual charge repulsion causes a force directly opposite to the surface tension. As the intensity of the electric field is increased, the hemispherical surface of the fluid at the tip of the capillary tube elongates to form a conical shape known as the Taylor cone. With increasing field, a critical value is attained when the repulsive electrostatic force overcomes the surface tension and a charged jet of fluid is ejected from the tip of the Taylor cone. The discharged polymer solution jet undergoes a whipping process wherein the solvent evaporates, leaving behind a charged polymer fiber, which lays itself randomly on a grounded collecting metal screen. In the case of the melt the discharged jet solidifies when it travels in the air and is collected on the grounded metal screen.
Nanofibers have the potential of numerous applications including high efficiency filter media and several uses have been made of these ultrafine fibers for filtration[xivxvxvixvii].
Within the last few years there has been an explosive growth in published reports on the use of electrospinning as a method of generating materials for biomedical applications.
Synthetic and semi-synthetic polymeric materials were originally developed for their durability and resistance to all forms of degradation, including biodegradation. Nanotechnology has the potential to revolutionize many sectors, including pharmaceuticals, information technology, medical devices, materials science, chemicals, and energy. Nanofibres provide a connection between the nanoscale world and the macroscale world, since their diameters are in the range of 1 to 100 nanometres and several metres in length. Therefore, the current emphasis of research is to exploit such properties and focus on determining appropriate conditions for electrospinning various polymers and biopolymers for eventual applications including: multifunctional membranes; biomedical structural elements (scaffolds used in tissue engineering, wound dressing, drug delivery, artificial organs, vascular grafts)[xviiixixxxxxi]; protective shields in specialty fabrics; and filter media for submicron particles in the separation industry.
The aim of this study is to investigate the efficiency of nanofiber coated onto nonwoven membrane in the reduction of the pore size, since this parameter seems to be a limit for their application in MBR.
The nanofiber webs were produced by means of an electrospinning prototype designed and constructed by TTX. Two different configurations of the machine were realised in order to optimise the production of the nanofiber webs (Figure 7). In fact, the first configuration allowed the production of nanoweb in a static way (plate collector), whilst the second one allowed the production of the nanoweb in a continuous way (rotating drum collector).

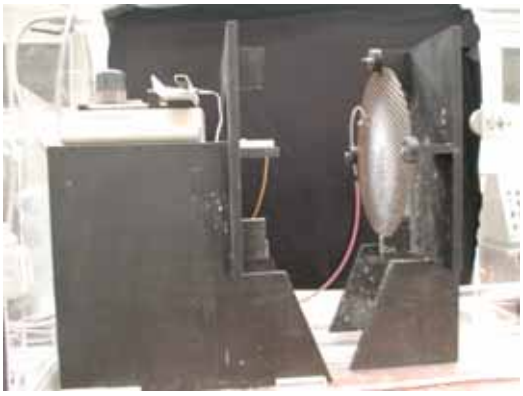
a)
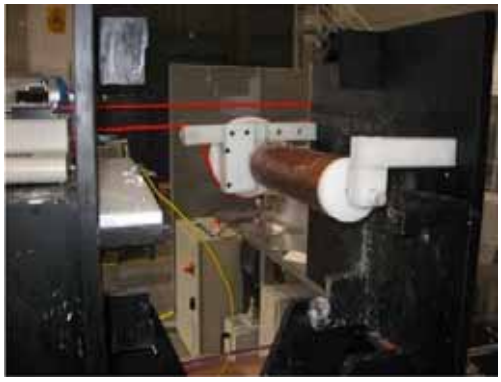
b)

Figure 7 - Configuration of the electrospinning prototype realised at TTX: a) first configuration; b)second configuration

The experimental campaign started with the first configuration.
Working conditions were optimised in terms of:

- Flow rate in the range 1 – 7.5 ml/min
- Polymer concentration (%wt) 14 – 24 %wt (step 2 %wt.)
- Distance between the electrode in the range 5 – 16 cm
- Voltage in the range 10 – 50 kV (step 5 kV)
- Number of syringes 1 – 4.

The electrospun polymer is nylon 6 (Sample ID NY6, Sigma Aldrich).
The performances of the nanofiber production were evaluated by means of SEM (scanning electron microscope) analysis. The mean diameter of the produced nanofiber was evaluated.

The nanoweb was then coated by means of the electrospinning prototype in the first configuration applying the optimised parameters onto two different textile membranes (PA_25 µm and PP_25 µm, produced by TTX) as reported below (Table 3):

Table 3 – Deposition conditions for Nylon 6 onto PP and PA non woven membranes

Sample ID	Electrospinning conditions
PA_NY6	nylon 6 nanofiber coating produced at: Voltage 25 kV; electrode distance 9 cm; flow rate 5 ml/min; polymer concentration 18% wt
PP_NY6	nylon 6 nanofiber coating produced at: Voltage 25 kV; electrode distance 9 cm; flow rate 5 ml/min; polymer concentration 18% wt

The optimised conditions were applied on the second configuration and were optimised for the production of the nanofibers in continuous way.
A study for the optimised of the flow rate in the condition optimised for the first configuration was carried out (Table 4).

Table 4 – Treatment conditions for production of nanowebs with the second configuration

Sample ID	Voltage [kv]	Distance between electrode [cm]	[nylon 6] [% wt.]	flow rate [ml/min]
NY6_DRUM_5.0	25	9	18	5.00
NY6_DRUM_2.5	25	9	18	2.50
NY6_DRUM_1.5	25	9	18	1.50
NY6_DRUM_1.0	25	9	18	1.00
NY6_DRUM_0.75	25	9	18	0.75
NY6_DRUM_0.5	25	9	18	0.50
NY6_DRUM_0.25	25	9	18	0.25
NY6_DRUM_0.10	25	9	18	0.10

The optimised working conditions were then applied for the deposition of the nanoweb onto nonwoven membranes used for water filtration.
The nanofiber coated membranes were then characterised in terms of physical properties – pore size, roughness, tensile strength - and filtration performances including bio-growth formation.

Textile Bioreactor (TBR)

A small scale was build and operated at TUB (Figure 8). The textile module was manufactured by A3 Water Solutions and consists of eight plates with a total filtration area of 0.24m². The module is submerged in a 32L tank (0.89m*0.2m*0.18m – 25L sludge volume) and aerated by a perforated membrane. In order to obtain an airlift loop circulation with higher velocities in the reactor the module was equipped with a top piece for additional rising hight (Figure 9 b). The permeate is withdrawn by a peristaltic pump (Ecoline, Ismatec, Wertheim-Monfeld, Germany) and recirculated in the reactor. Pressure and flux are measured online after the membrane module.

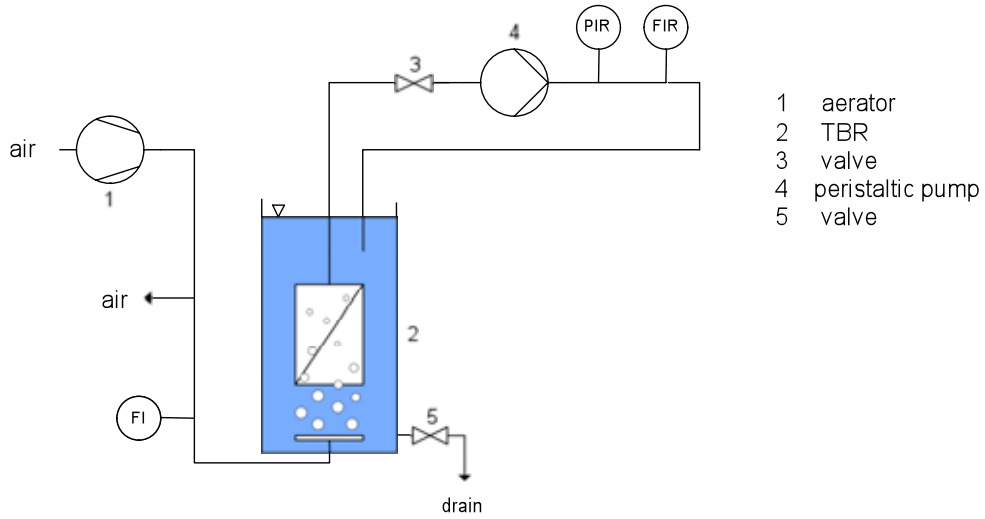

Figure 8 - Flowsheet of TBR

The sludge was taken from the AMEDEUS pilot plant operated within WP2 on ground of a pumping station in Berlin city center. The system was feeded twice a day with synthetic wastewater according to DIN EN ISO 11733 in a quantity to ensure similar sludge load as in the pilot system. The module was operated in a filtration/relaxation modus of 8min/2min.

a b c

Figure 9 – Textile module (a); module with top piece (b) and TBR (c)

3 Results and Discussion

3.1 Membrane characterisation

3.1.1 FT-IR analysis.

FT-IR analyses were performed to investigate the composition of the commercial membranes collected by the partners (TUB and KWB) for the characterisation. Tests assessed on different samples showed that the raw materials used to realise textile membranes for filtration application are principally three (Table 5):

- Polyethylene (PE) at High Molecular weight or at Ultra High Molecular weight
- Polypropylene (PP) High Density
- Polyamide (PA), both Nylon 6,6 and Nylon 6,12.

Table 5 – Polymer used for the production of investigated non woven membranes

Sample ID	Raw materials
A3 membrane	PVDF/PET
PA_5mm	Nylon 6
PA_10mm	Nylon 6
PA_15mm	Nylon 6
PA_24mm	Nylon 6
PP_10mm	Polypropylene
PP_15mm	Polypropylene
PP_24mm	Polypropylene
PP_50mm	Polypropylene
POLYNOVA	-
SFT_10mm	Nylon 6:12
SFT_1mm	Nylon 6:12
SEFAR	Nylon 6:12
Chaussette	Polyethylene HMW
2325990502	Polyethylene HMW
16P05A Solupor	Polyethylene UHMW
E-9H01A Solupor	Polyethylene UHMW
E-9H06A Solupor	Polyethylene UHMW
Viledon FF 2007	Polypropylene

These analyses confirmed that the choice of the polymer for the production of new textile membranes by means of Melt Blown technology performed in TTX was correct.
Both polymers were selected since they are the cheapest ones in comparison with other materials used for the production of the membranes such as Polyvinylidene fluoride (PVDF), Polyethylene terephtalate (PET) or polytetrafluoroethylene (PTFE).

3.1.2 Thermal Gravimetric Analysis (TGA)

TGA analyses showed that tested material showed a high thermal resistance since for all samples the degradation temperature is higher than 370 °C. Tests were performed in wet condition to simulate working condition (they have to be applied in submerged plants) and to evaluate the wettability of selected materials (Figure 10) in comparison with the control membrane (A3 membrane).

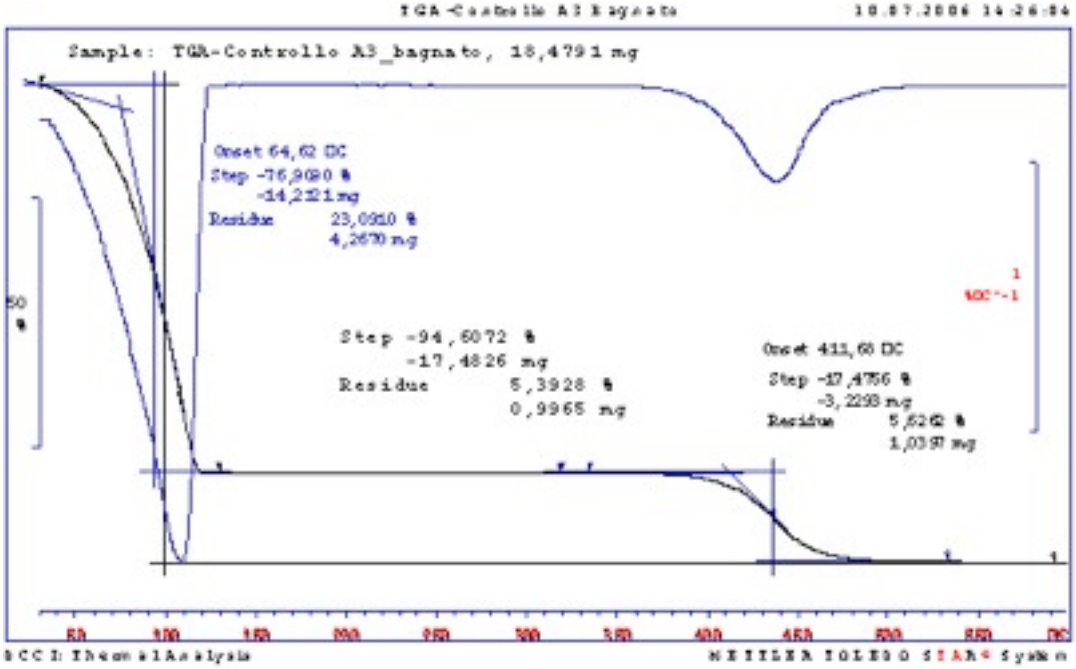

Figure 10 – Thermal Gravimetric Spectrum concerning water desorption (peak onset at 64 °C) and decomposition (peak at 411 °C) of A3 membrane (control).

The results are listed in the Table 6:

Table 6 – Wettability and degradation temperature for the selected materials

Raw materials	Wettability [%wt]	Degradation Temperature [°C]
PVDF/PET	76.91	411.68
Polyamide (PA)	87.77	379.74
Polypropylene (PP)	66.11	442.96
Polyethylene (PE)	63.31	453.21

It's interesting to note that the olefins (PE, PP) have a lower capability to absorb water in comparison with the PET and PA because of the chemical composition of the polymers; in fact, PA and PET have some polar species in the polymer chains, such as carboxylic or amino groups able to form low energy linkage (Van der Waals forces or Hydrogen bonds) with water molecules. This outcome suggests that probably the wettability of selected materials have to be changed to reach the performances ensure by the control within Task 1.3.

3.1.3 Chemical Resistance to acid (HNO_3, 1 M at pH < 2); to alkali (NaOH, 1 M at pH > 12); to chloride (NaOCl, 1000 ppm) and to hydrogen peroxide (H_2O_2, 500 ppm).

One of the most important property which has to be ensured by textile membranes is the chemical and mechanical resistances of the membranes in each step of the MBR process.
Gravimetric analyses showed that the membranes showed a different behaviour according to the material used to produce them (Figure 11):

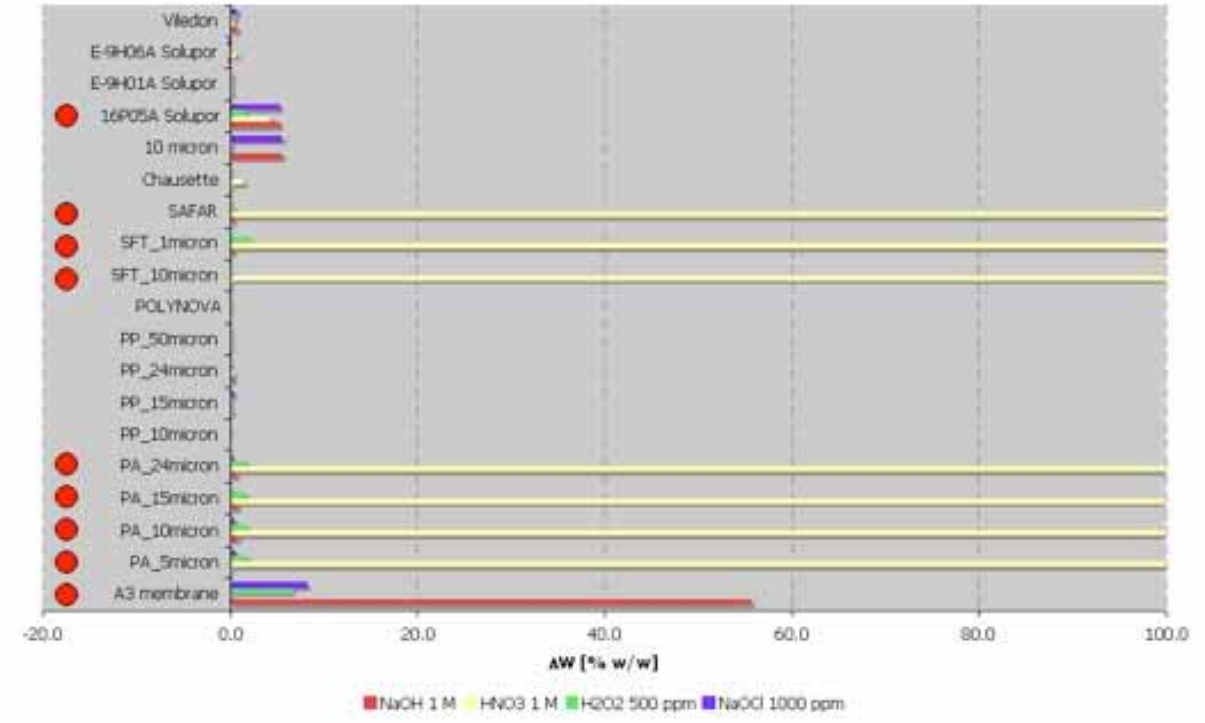

Figure 11 – Gravimetry analyses of the studied membranes in the different solution selected according the internal standard test extracted from ISO1817.

This analysis showed that all polyamide membranes are affected by the acid solution; in fact after this treatment the nylon membranes are completely destroyed. On the contrary, the olefin membranes, both polyethylene and polypropylene, are not sensitive to the different treatments and they are the most stable in tested conditions.
It's interesting to note that also the A3 membrane is sensitive to the applied solutions: the alkali solution promote a decomposition of the PET and a degradation of the PVDF that produce a loss of weight higher then 50%wt. This outcome is probably due to the strong treatment conditions that were selected, since literature does not report a Standard Test method specific for membrane application.
The study of the mechanical properties of the untreated membranes in comparison with the treated ones confirms the previous results (Figure 12;
Figure 13)

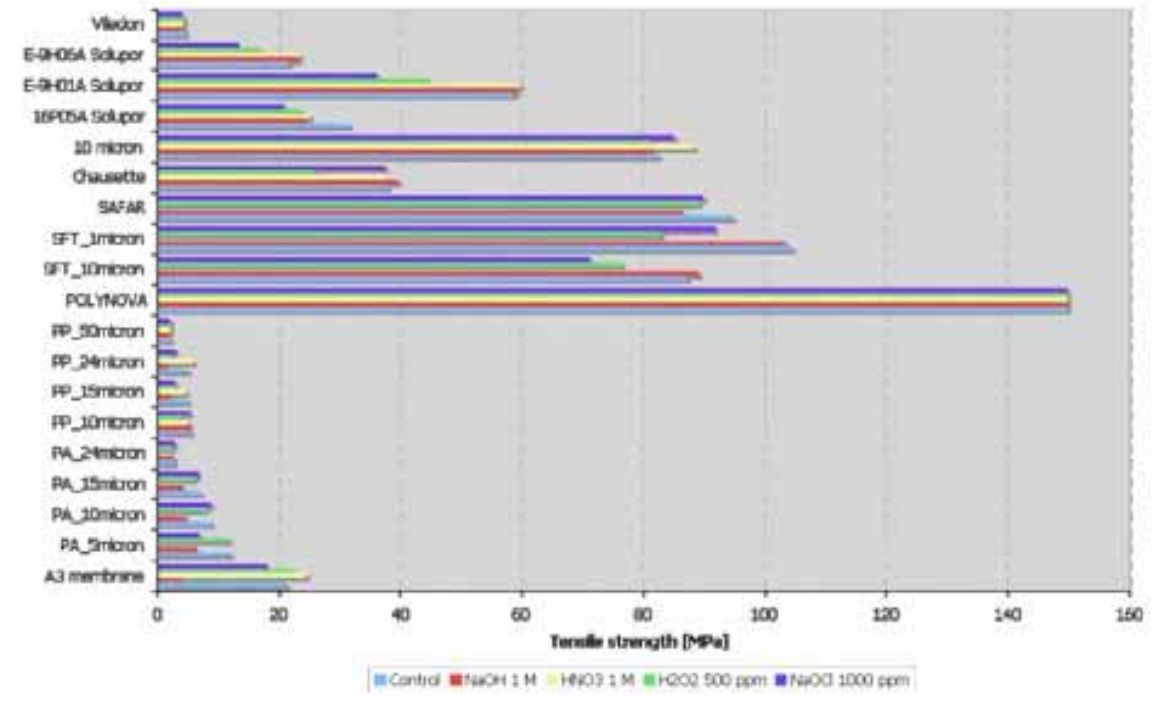

Figure 12 – Tensile strength measurements of the studied membranes in comparison with the untreated ones (control).

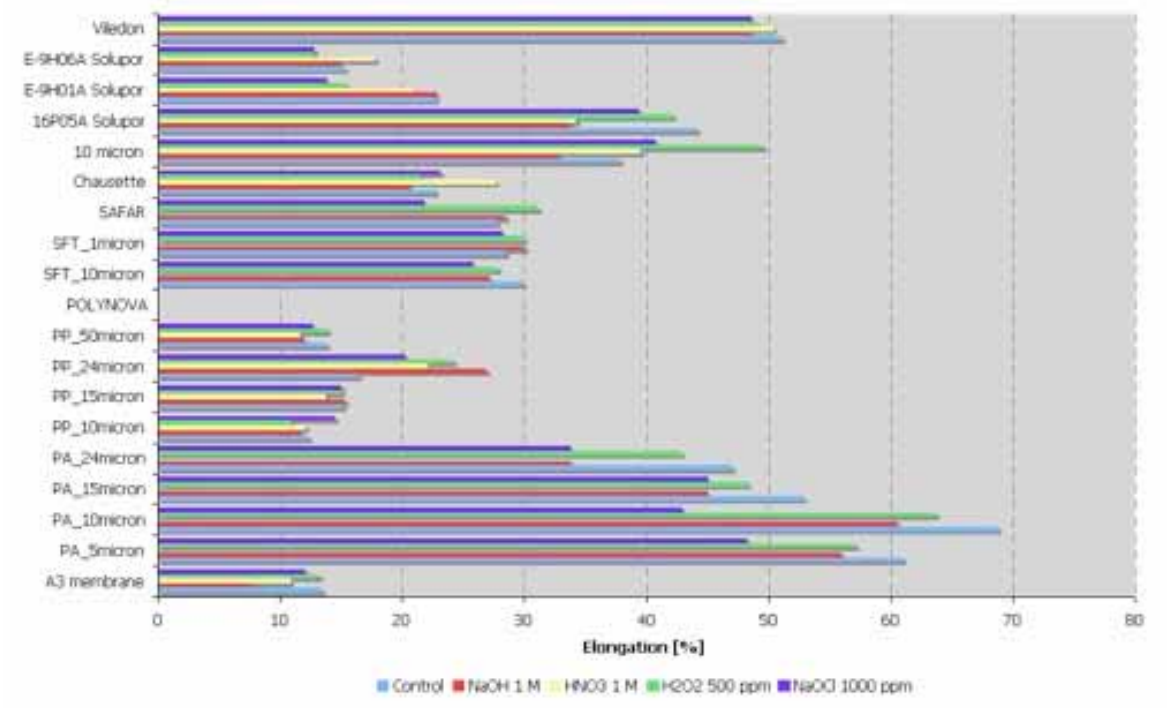

Figure 13 - Elongation measurements of the studied membranes in comparison with the untreated ones (control).

The tensile strength measurements confirm that the polymers are affected from the treatments in a different way as reported for the gravimetric analysis. It was found also that the structure of the textile membranes and the width affects the mechanical properties of the substrates. The highest performances were ensured by the POLYNOVA membranes for whom the highest tensile strength and elongation values were found. This is due to the characteristic of the membranes; the properties seem to be due to the PP coating applied on the surface.

To verify if the changes in the mechanical properties were due only to a degradation of the polymer chains or also to a modification of the arrangement of them in the space, DSC analyses were carried

out. As well known, changes on the distribution of the polymer chains induce changes in the crystallinity of the matrices, which is proportional to the melting enthalpy (ΔH_m).
In the following tables (Table 7) the values of the ΔH_m for the different material in the tested solution.

Table 7 – DSC analysis on tested materials in terms of melting enthalpy

NaOH 1M - pH > 12			HNO_3 1M - pH < 2		
Material	Melting point [°C]	$\Delta(\Delta H_m)$ [%]	Material	Melting point [°C]	$D(DH_m)$ [%]
PVDF	169	-4.13	PVDF	169	50.71
PET	260	29.27	PET	260	7.61
Nylon 6:6	263	3.22	Nylon 6:6	263	N.A.
PP	166	4.24	PP	168	-0.58
Nylon 6:12	255	-1.93	Nylon 6:12	255	N.A.
Nylon 6:12	255	-9.02	Nylon 6:12	255	N.A.
HMW PE	140	1.98	HMW PE	140	-0.57
UHMW PE	140	5.98	UHMW PE	140	2.40
H_2O_2 - 500 ppm			NaOCl - 1000 ppm		
Material	Melting point [°C]	$\Delta(\Delta H_m)$ [%]	Material	Melting point [°C]	$D(DH_m)$ [%]
PVDF	169	6.03	PVDF	169	27.54
PET	260	1.12	PET	260	13.20
Nylon 6:6	263	21.37	Nylon 6:6	263	6.59
PP	168	17.06	PP	168	4.57
Nylon 6:12	255	8.20	Nylon 6:12	255	5.39
Nylon 6:12	255	-3.03	Nylon 6:12	255	-2.14
HMW PE	140	6.34	HMW PE	140	1.47
UHMW PE	140	24.91	UHMW PE	140	8.82

DSC analysis suggested that only the degradation of the polymer chains induced by depolymerisation reaction promoted by hydrolysis catalysed by acid or alkali for the polycondensation polymers, such as PET and PA, or with free radical for the olefin. So the reduction on ΔH_m is not due to changes in the crystallinity. On the contrary the change on melting enthalpy for PVDF after the treatment with acid (HNO_3, 1M) is probably induced by the modification of the crystalline structure induced by the interaction of nitric acid with the fluorinated groups[xxii]. In any case, PET seems to be responsible for mechanical properties since no differences were recorded respect to the untreated A3 membrane.

3.1.4 Roughness measurements

Filtration performances of the membranes are affected by the superficial characteristic of the filters: in fact, a smooth surface reduces trapping of the particles that induce a higher retention, leading to lower flux[xxiii]. For this reason, an evaluation of the roughness of the selected membranes was carried out. In Table 8 the results of the analysis were reported.

Table 8 – Roughness values for all tested textile membranes

Polyamide porosity [µm]	Side	Sa	Sq	Ssk	Sku
5	**A**	**7.60**	**9.93**	**-0.271**	**2.04**
	B	**7.34**	**10.1**	**-0.401**	**2.13**
10	A	12.5	15.3	-0.209	1.84
	B	10.6	16.6	-0.622	2.64
15	A	14.5	16.1	-0.339	1.86
	B	15.8	18.5	-0.52	2.57
24	A	18.4	21.2	-0.303	1.87
	B	21.8	27.6	-0.343	2.07
Polypropylene porosity [µm]	Side	Sa	Sq	Ssk	Sku
10	A	27.8	37.2	0.52	3.43
	B	10.6	16.4	-0.8	3.89
15	A	20.7	27.4	-0.082	2.87
	B	17.5	16.3	-0.345	2.64
25	A	33.2	45.6	-0.64	3.27
	B	60.6	83.1	-0.17	2.8
50	A	43	56	-0.432	2.13
	B	27.8	39.8	1.78	3.54
Commercial Membrane	Side	Sa	Sq	Ssk	Sku
A3 (control)	**A**	**1.50**	**1.95**	**0.381**	**2.01**
	B	**5.73**	**6.10**	**-0172**	**1.82**
POLYNOVA	A	76	122	0.183	6.3
	B	69	131	0.827	6.8
SFT 1 µm	A	27.8	32	-0.389	1.96
	B	28.2	34.2	-0.72	2.9
SFT 10 µm	A	18.7	26.7	-0.42	1.79
	B	17.4	22.9	-0.382	2.06
Chausette	A	3.11	3.76	-0.0256	1.73
	B	3.41	4.12	-0.089	1.95
SEFAR	A	28.1	33.4	-0.66	3.48
	B	26.8	32.9	-0.61	3.28
Viledon FF2007	A	11.5	20.1	0.071	1.52
	B	6.13	8.18	0.0363	3.43
2325990502	A	16.7	14.2	-0.426	3.05
	B	18.7	19.4	-0.504	5.94
Solupor 16P052A	**A**	**1.42**	**1.82**	**-0.061**	**1.44**
	B	**1.54**	**2.08**	**-0.0159**	**1.28**
Solupor E9-H01A	**A**	**1.95**	**2.54**	**-0.096**	**1.44**
	B	**1.77**	**1.92**	**-0.0272**	**1.61**
Solupor E9-H06A	**A**	**1.92**	**2.18**	**-0.00172**	**1.36**
	B	**1.64**	**1.88**	**-0.059**	**1.21**

The parameters reported in the table below are all amplitude parameters. Some parameters are listed in the EUR 15178 EN report. All these parameters are defined in comparison with a mean plane obtained through levelling of the mean square plane of the measured surface and then through centring of heights around the mean.

Sa : arithmetic mean of the deviations from the mean. This parameter is included in the EUR 15178 EN report.

Sq : quadratic mean of the deviations from the mean. Computes the efficient value for the amplitudes of the surface (RMS). This parameter is included in the EUR 15178 EN report.

Ssk : Symmetry of the distribution curve of depths. A negative Ssk indicates that the surface is composed with principally one plateau and deep and fine valleys. In this case, the distribution is sloping to the top. A positive Ssk indicates a surface with lots of peaks on a plane. The distribution is sloping to the bottom. Due to the big exponent used, this parameter is very sensitive to the sampling and to the noise of the measurement. This parameter is included in the EUR 15178 EN report.
Sku : Flatness of the distribution curve of depths. Due to the big exponent used, this parameter is very sensitive to the sampling and to the noise of the measurement.

The results suggested that for the textile membranes the surface has the same smoothness in both sides (A and B) whilst the control one (A3 membrane) shows a different behaviour depending on the tested side, because of the two components making the substrate.
In any case, textile membranes seem to have a higher roughness in comparison with the conventional membranes because of their fibrous structure. The highest values is recorded for POLYNOVA membranes since the coated textile is affected by the weaving of the yarns and by the coating applied on it. This outcome suggests that the best textile substrates to use as membrane are nonwovens; in fact, Polyamide 5 µm membrane produced by TTX with Melt-Blown technology shows a smoothness quite similar to the conventional ones, so by optimising the production parameters we should reduce the roughness.
It's interesting to note also that the Nanofiber membranes produced by Solupor have a roughness comparable with the one recorded for the control. This is due to the nanofibers webs deposited on the surface or to the fact that it's obtained by casting and not by textile processes. In fact, it was found that these membranes are stretched membranes, different from the conventional textile ones.

3.1.5 Capillary Flow Porometry

The pore size of a filter is the average pore dimension through which the fluid must pass. The smaller the pore, the more efficient the filter media will be, enabling it to remove smaller particles.
The pore size of the tested membranes was investigate in order to evaluate the performances of the newly realised membranes and to know the real pore size of the commercial ones.
Measurements made on textile membrane (PA 5µm, produced by TTX) using capillary flow porometry are presented in Figure 14.
The dry curve represents data obtained with a dry sample and the wet curve corresponds to data from the wet sample. The half-dry curve is not measured. It is calculated from the measured dry curve to yield half of the flow rate through dry sample at a given differential pressure. The use of half-dry curve for the determination of mean flow pore diameter is discussed below.
It is shown later that Pore diameter is calculated from differential pressure and a number of other pore characteristics are computed from these data.
The pressure required to test nonwovens is usually very low. For the sample used in this study, the pressure required is less than one psi.

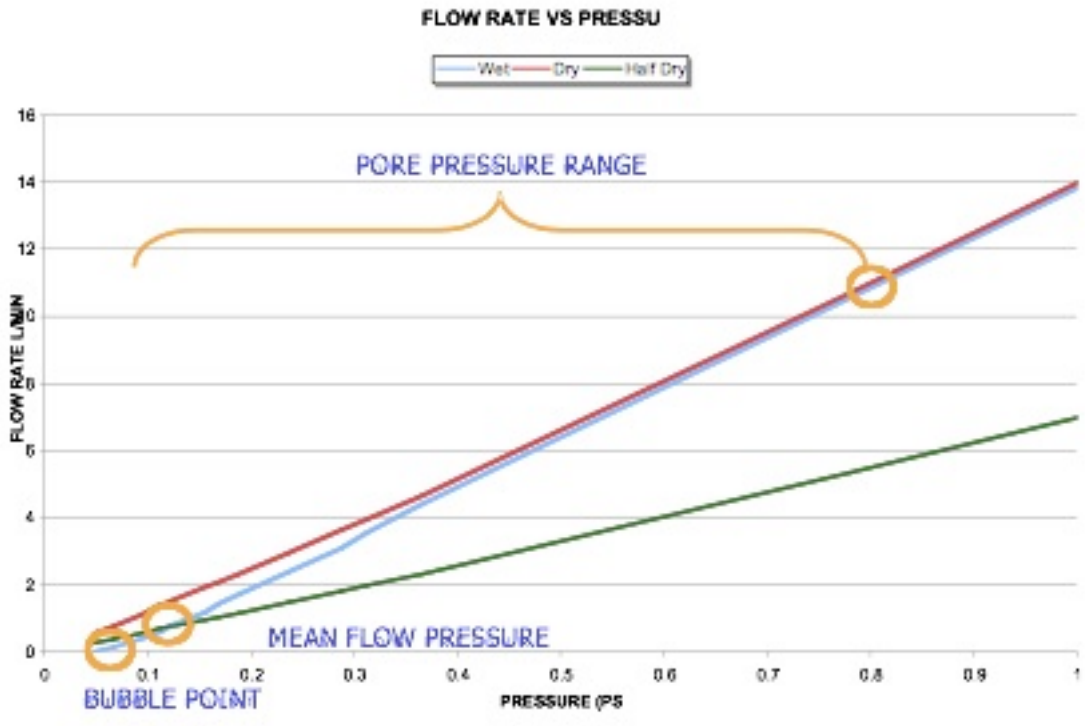

Figure 14 - Differential gas pressures and gas flow rates through sample PA 5µm

The diameter of a pore normally changes with pore path. The instrument detects a pore by sensing flow through the pore. Equation 4 suggests that differential pressure required to displace liquid in the pore is inversely proportional to pore diameter. Therefore, pressure required to displace liquid in a pore would be the highest at the most constricted part of the pore. Once this highest pressure is reached, liquid from the rest of the pore will be removed, gas will start flowing through the pore and the instrument will detect the presence of the pore. Since the measured pressure is the pressure required to displace liquid at the most constricted part of the pore, the calculated pore diameter is the diameter of the pore at its most constricted part. Consequently, all pore diameters measured by extrusion flow porometry are constricted pore diameters.

The largest constricted pore diameter[xxiv]: The largest pore should open up at the lowest pressure. Therefore, the pressure, at which flow starts through the wet sample (bubble point) is accurately determined and the pore diameter calculated from this pressure is the largest constricted pore diameter of all pores. The data in Figure 14 yields a value of 13.09 µm. The largest pore diameter gives the smallest particle that can be separated.

The constricted mean flow pore diameter: The mean flow pore diameter is such that fifty percent of flow is through pores larger than the mean flow pore diameter and the rest of the flow is through smaller pores. The mean flow pore diameter is obtained from the mean flow pressure corresponding to the intersection of wet curve and half- dry curve. The data in Figure 15 yield a value of 5.28 µm. Mean flow pore diameter is normally a measure of the size of majority of pores and fluid permeability.

Constricted pore diameter range: The bubble point pressure and the pressure at which the dry and wet curves meet yield the pore diameter range. The pore diameter range determines the barrier and flow properties of the membrane.

Flow distribution over pore diameter[xxv]: The pore distribution is presented in as the distribution function, f:

$$f = - d (Fw / Fd) \times 100) / dD \quad (5)$$

where Fw and Fd are flow rates through wet and dry samples respectively at the same differential pressure. The distribution function is such that area under the curve () in a pore diameter range is the percentage flow through pores in that range. The distribution shows that the material has a trimodal distribution. Nevertheless, the pores are in the range of about 1 to 6 µm and the rest of the pores are negligible. It has been shown that this distribution is close to the pore fraction distribution.

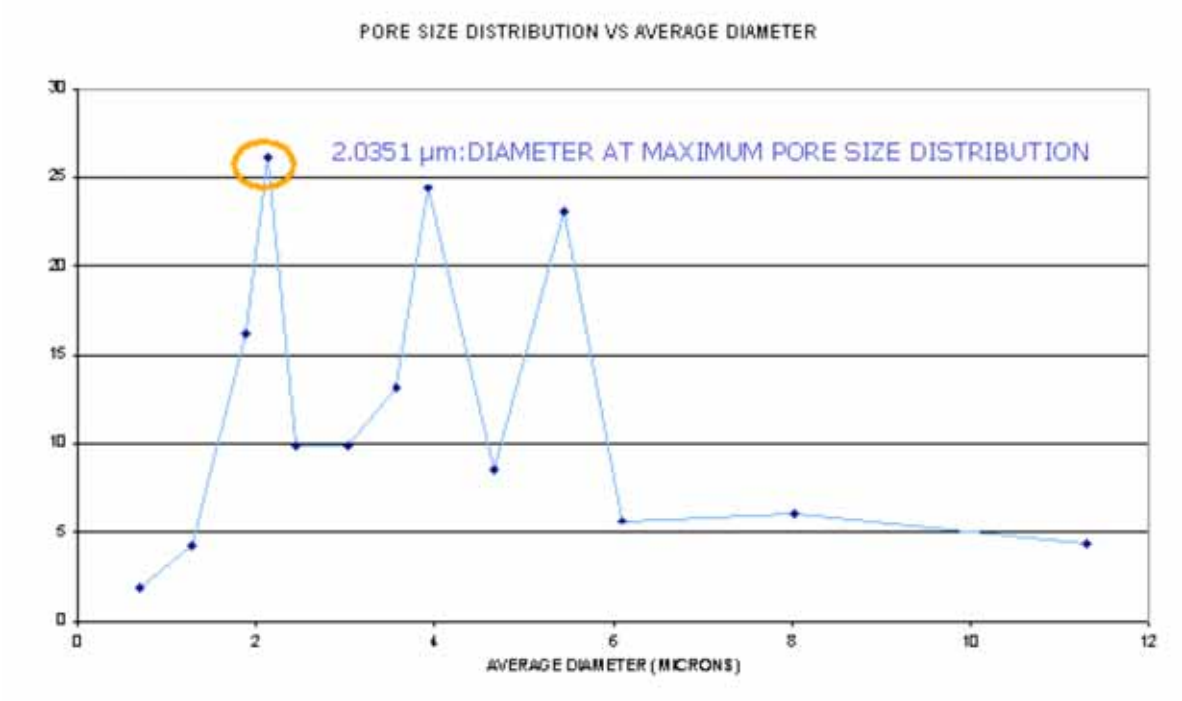

Figure 15 - Pore distribution obtained from data in Figure 9.

In Table 9 are listed the mean diameters and standard deviation values from the mean for all tested membranes:

Table 9 - Mean diameter and Standard deviation for all tested membranes

Sample ID	Porosity	
	Mean Diameter [μm]	SD [μm]
A3 membrane	0.294	0.1404
PA_5μm	5.285	3.4761
PA_10μm	10.169	6.5336
PA_15μm	15.5128	10.6223
PA_24μm	23.1887	19.2739
PP_10μm	9.5247	6.5243
PP_15μm	15.1656	12.1807
PP_24μm	25.21	16.4866
PP_50μm	49.7782	42.5107
POLYNOVA	64.6779	65.2361
SFT_10μm	19.7934	16.0704
SFT_1μm	9.6585	8.3199
SEFAR	9.1838	7.9798
Chaussette	2.9600	0.3800
2325990502	19.4800	0.4692
16 P05A Solupor	0.3300	0.0737
E-9H01A Solupor	0.4700	0.1340
E-9H06A Solupor	0.4300	0.3035
VILEDON FF 2007	10.9000	0.9774

The main results are the following:

- SFT membranes showed a larger pore size in comparison with the nominal one.
- As expected, textile membranes have a larger mean pore size then the conventional one (A3 membrane) except for the Solupor membranes even if further investigations on those are needed, to verify the nature of these membranes.
- By increasing mean pore size, the distribution of the pores became narrower.
- Tested samples, including control, have a multimodal distribution of the pores.

3.1.6 Filtration performance

The reference material, a 0.2µm PVDF membrane was tested on two different days in order to see a possible change in the sludge and the resulting filterability. As can be seen in Figure 16, the initial flux, the dynamics of the flux decline and the resulting stationary flux after two hours were quite comparable for the two trials. The filterability tests with the different textiles were accomplished within two weeks. It can be concluded that the sludge and filterability properties did therefore not change too much.

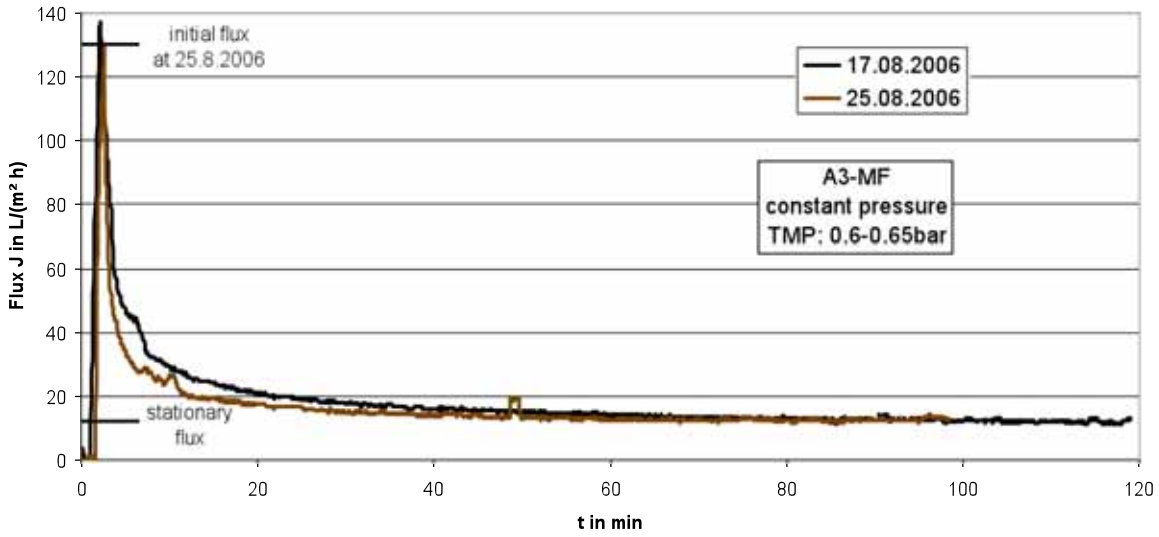

Figure 16 - Flux decline for the membrane on two different days

In Figure 17 the stationary flux is showed for the different textiles in comparison to the reference membrane. Most textiles have a flux between 5 and 11 L/(m²h) and have therefore a poorer filtration performance than the membrane (12 L/(m²h)). The DSM filtration media shows better performance for pore sizes between 0.3µm and 0.5µm. This is especially surprising as higher fluxes were assumed for larger pore sizes while probably having a worse retention. Textiles which produced a very turbid permeate were not included in the graphs.

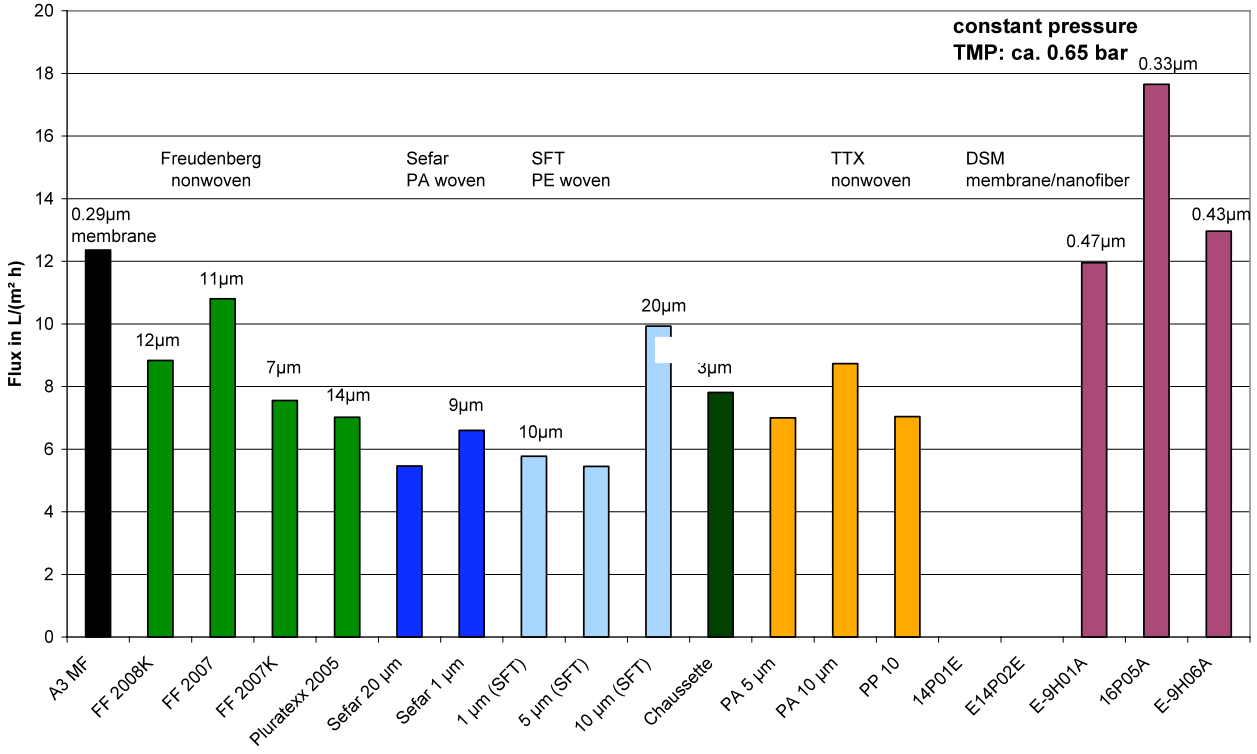

Figure 17 - Stationary end flux after two hours filtration

As can be seen in Figure 17 the initial fluxes were much higher for most textiles in comparison to the membrane and the media from DSM. It can therefore be assumed that the high initial fluxes cause a severe fouling of the filtration textile or a cake build-up and are a cause for the much lower stationary fluxes. This problem might be solved by constant flux conditions and low fluxes.

In order to further characterize the textiles, the critical flux was determined in the filtration test cell. The critical flux gives an impression up to what fluxes the filtration can be driven without risking severe fouling (Table 10).

Table 10 - Critical flux for different textiles

Filtration media	critical flux between L/(m²h)	mean value in L/(m²h)
Control	12.2-14.5	13.4
FF 2007 (Sample ID: A4)	8.2-11.3	9.8
E-9H01A (Sample ID:H1)	10.2-13.1	11.6
16P05A (Sample ID:H4)	12-14.6	13.3

As can be seen in Table 10 the critical flux is highest for the membrane and filtration media H4. While the critical flux is slightly smaller for H1 it is much smaller for textile A4.

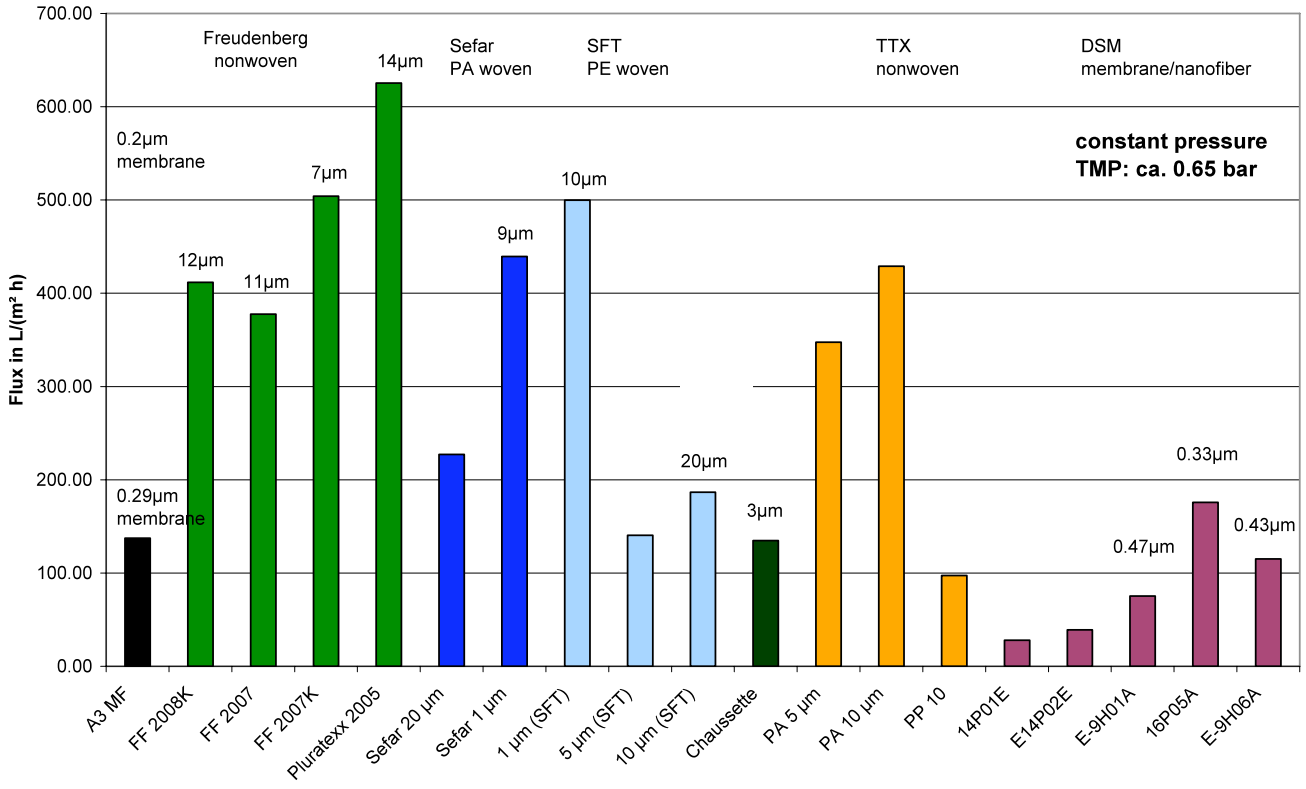

Figure 18 - Initial flux for tested membranes

3.1.7 Long term filtration tests

Figure 19 shows the filtration performance with the reference microfiltration membrane. No TMP increase can be observed during a 12h filtration. The flux was set to 15-16 LMH. So this is higher than the critical flux given in table 2. The experiments for the textiles A4, D1, G1 and G2 are shown from Figure 20 to Figure 23. These experiments were not conducted the planned 10-12 hours due to the very high filtration resistance and the resulting strong increase in TMP. In all cases the permeate chamber was sucked empty by the permeate pump. The results received with the novel filtration material from producer H are shown in Figure 24 and in Figure 25. Though material H4 also showed an increase in TMP the tests could be conducted during a period of approx. 11h. Material H1 showed only a slight increase in TMP but generally a higher value of TMP than the membrane.

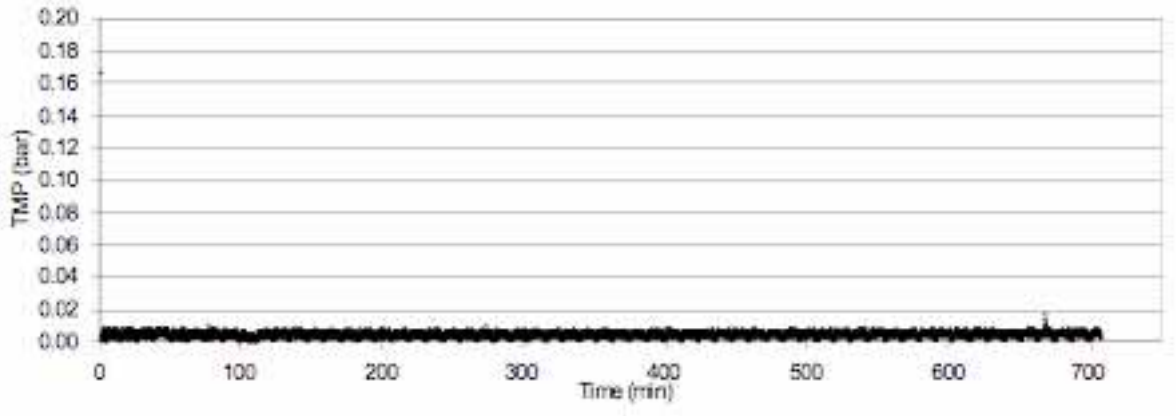

Figure 19 - results of the long term filtration with the reference membrane (PVDF, 0,2µm)

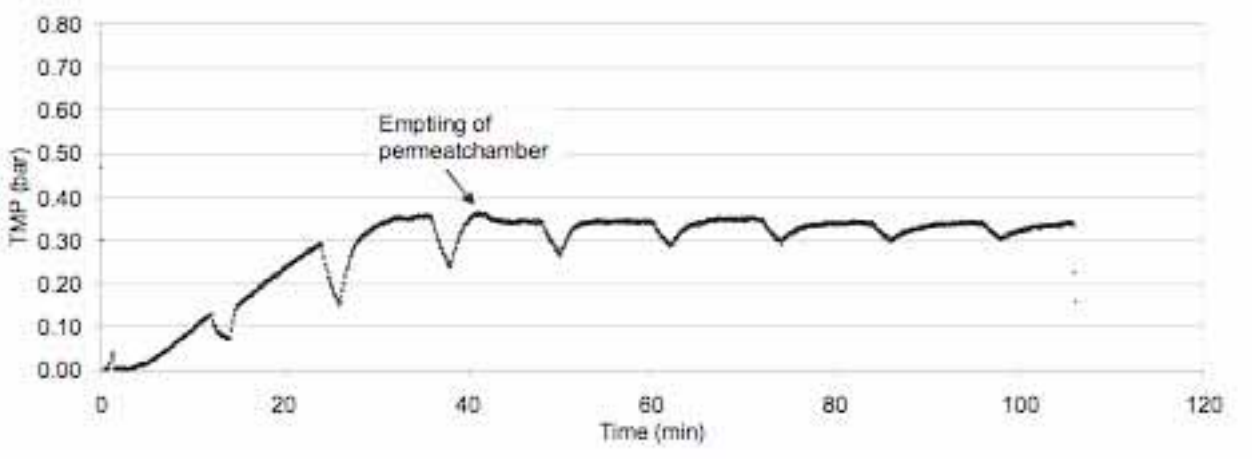

Figure 20 -TMP increase during long term filtration with nonwoven A4

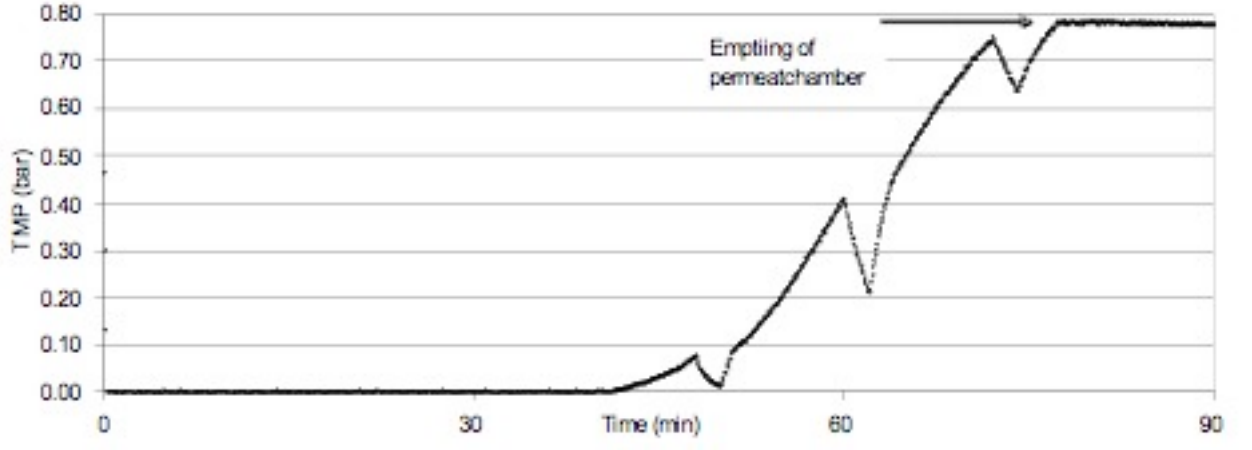

Figure 21 - TMP increase during filtration with D1 woven

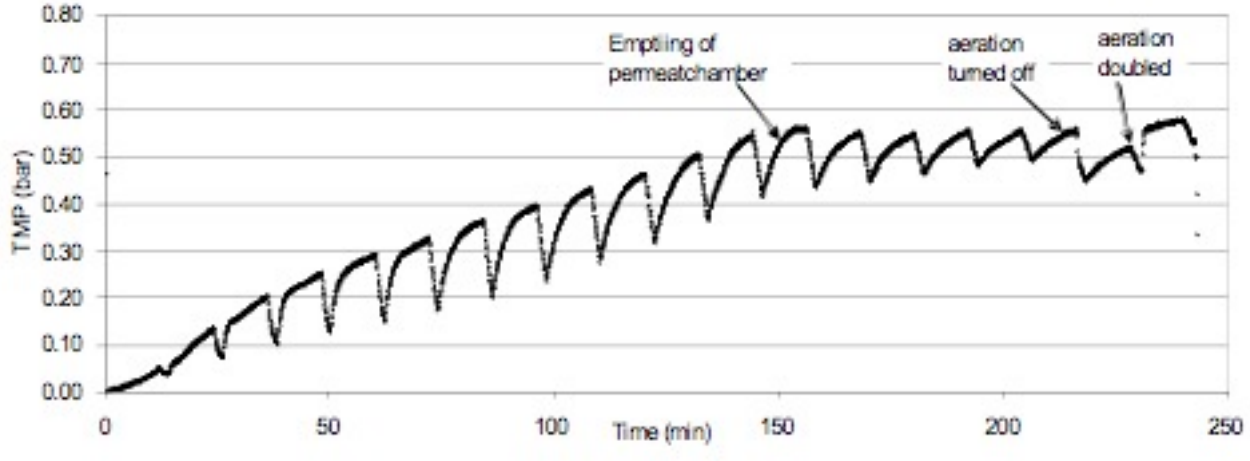

Figure 22 - TMP increase during filtration with non woven G1

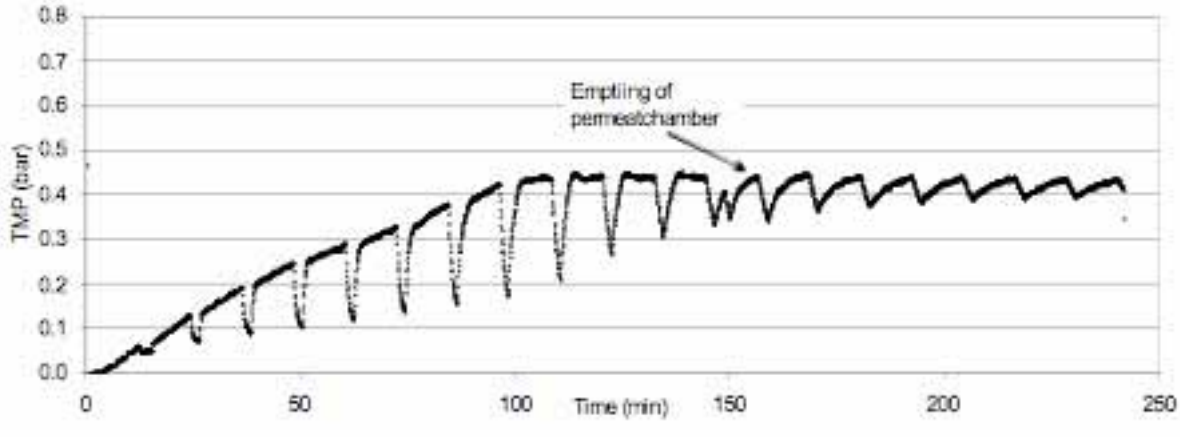

Figure 23 - Filtration performance of non woven G2

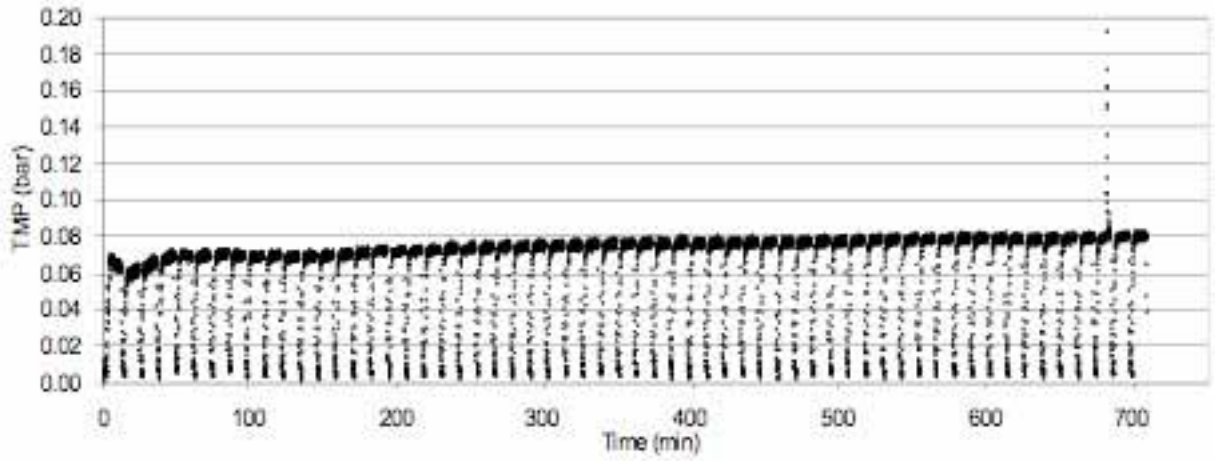

Figure 24 - Filtration performance of novel filtration media H1

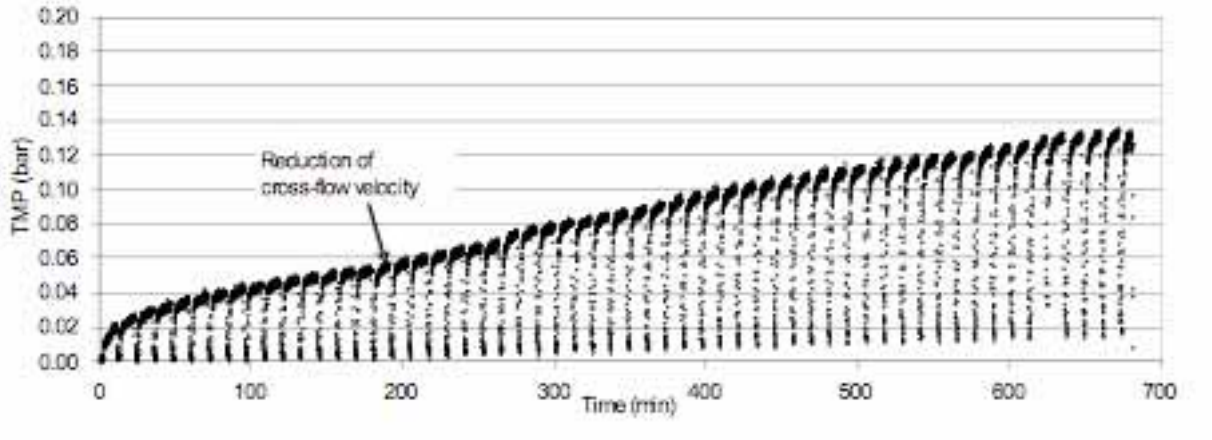

Figure 25 - TMP increase of novel filtration media H4

The results of the permeate analysis for polysaccharides, proteins and COD can be seen in Figure 26. In some cases the sample volume was not enough to do all determinations. In this cases the columns is missing. For the polysaccharides and proteins, elimination can be seen in all cases. For the COD in case of the woven D1, the COD of the permeate is higher than that of the centrifuged retentate, meaning that more biomass and components could be retained by centrifuging.

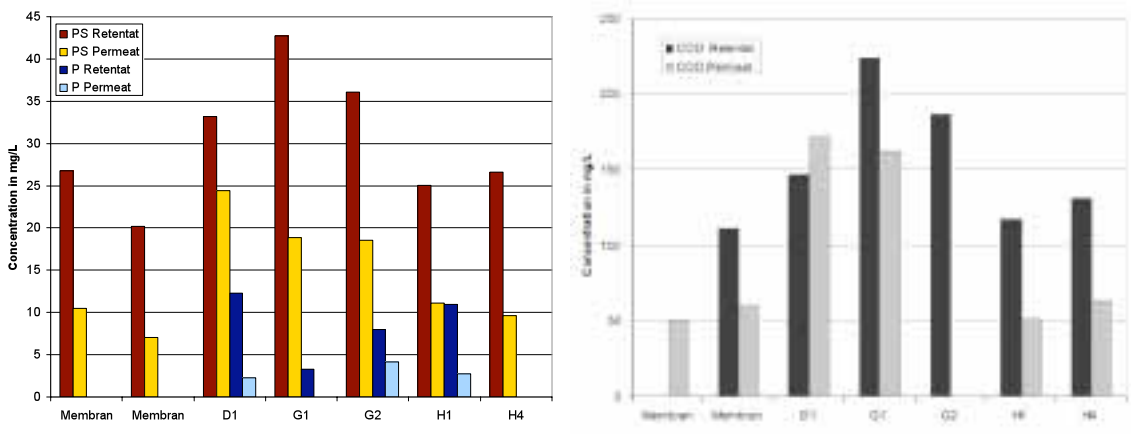

Figure 26 - Elimination of polysaccharides, proteins and COD

In Table 11, the turbidity of permeate and the number of colonies on a agar plate are reported. The very turbid permeates of the nonwovens A4, G1 and G2 and the woven D1 correlate normally with low COD retentions and a low hygienic standard. It must be said, that these samples were taken after a few hours of filtration. Due to the severe TMP increase the tests with these textiles were not conducted over the planned 10-12h.

Table 11 - Quality of permeat in terms of turbidity and hygienic aspects (sludge >500 colonies)

	Turbidity			
Membranel	**860nm**		**520 nm**	**Colonies**
	Concentration (FAU)	**Extinction**	**Extinction**	**dilution 10^{-3}**
Membran/Textil	---	-0.01	0.005	4
Membran/Textil	---	0	0.03	11
A4	56.57	0.04	0.113	
D1	+++	0.58	0.972	431
G1	51.58	0.04	0.125	
G2	+++	0.85	1.301	343
H1	---	0	0.011	2
H4	---	0	0.031	5

3.1.8 Optimisation of filtration parameters

In a first step the two used sludges were characterized. As can be seen in Figure 27 the studge from the small scale MBR 1) has a much worse filterability than the sludge from the AMEDEUS pilot 2). Kraume et al. (Kraume, M., Wedi, D., Schaller, J., Iversen, V.,Drews, A. (2007) Fouling in MBR – What use are lab investigations for full scale operation? IMSTEC 2007 (accepted), Sydney.) studied the differences between the operation of different scaled MBRs. They found that the energy input per m³ treated wastewater is strongly different between lab, pilot and full scale. The high energy input surely leads to much smaller flocs and thus to a denser filter cake and a worse filterability. As pore sizes of textiles are much larger than those of microporous membranes this is especially detrimental. The small flocs do not only form a dens filter cake but are also able to penetrate the textile and result pore clogging or low quality permeate.

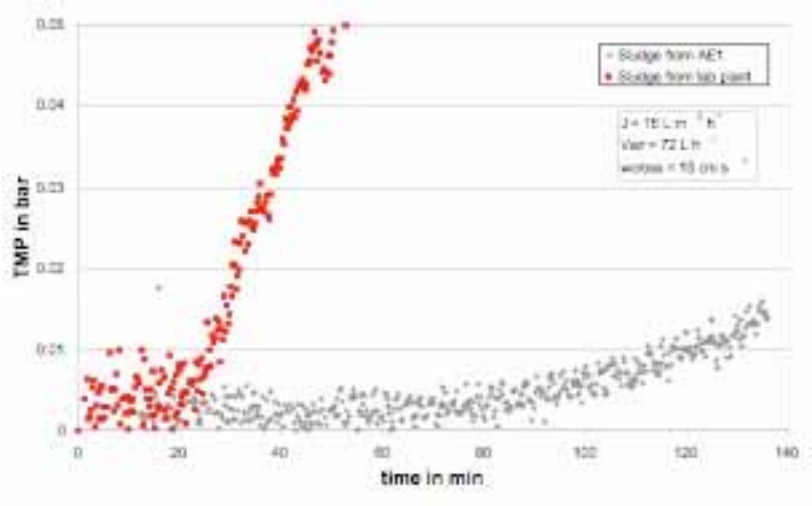

Figure 27 - Filterability of the two investigated sludges (Freudenberg nonwoven)

3.1.9 Adequacy of the non woven materials in MBR module

The tests carried out by on the non wovens PP_24μm and PA_24μm aimed to verify the adaptability of the non woven membrane material to the production processes used by the SME to construct their modules.

- *Strength*
  Test conducted on the strength of the commercial non woven membranes (both PP and PA) showed that they have a low mechanical resistance, as confirmed by the characterisation tests performed on non woven membranes during the first year of the project. In particular, the structure of the non woven membranes and their thickness seem to affect this parameter. PP and PA non woven membranes with closer structure and higher thickness were being produced by TTX.
  The design of new non woven membranes specific for the requirement of the project and the modification on filtration performances planned in collaboration with WP1 partners is in progress. Latest membranes to be still tested at A3 show a modification on porosity and roughness that for formerly tested materials were too high.
- *Desorption*
  By reducing treatment time a reduction of the desorption of water and organic solvent (acetone) could be also achieved. In fact, the tested non woven membranes showed very high desorption values:
  - PP: 400 ml/m²
  - PA: 350 ml/m²

  Up-scaled to a 70 m²-module, this stands for 30 l. 30l is definitely too much, drying of a module that shows this water desorption will be hardly possible, what causes bacteria and funghi fouling.
  Some improvement on the membrane structure and/or functionalisation of the surface by plasma could be suitable to affect this parameter.
- *Cushion-production*
  PP can be easily welded at standard-conditions (225°C, 30s), the connection is mechanically firm and acceptable for the further production process and MBR applications, but material elongates in production process. For PA, even a welding at minimum required temperature (160°C) melts and harms the PA material. An interconnection can be processed, but the requirements due to strength and tightness are not fulfilled because the material is partly destroyed at the changeover between welded and not welded membrane material (Figure 28). At this place, the highest mechanical force appear during operation.

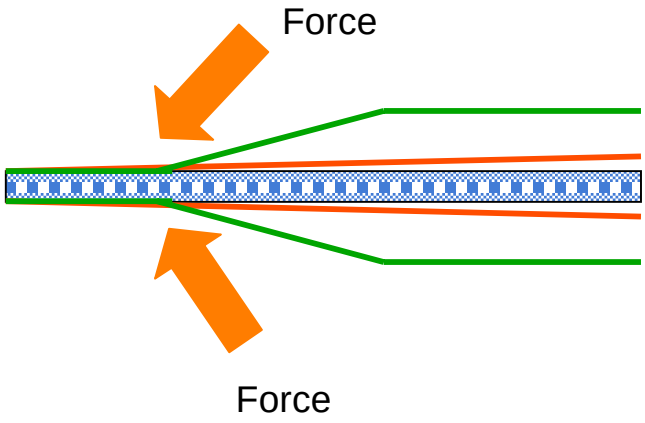

Figure 28 – Layout of the cushion production

These tests showed that PP is more suitable than PA for MBR application. To solve the elongation problem of the PP material, some possible solution will be discussed by TTX and A3.

- *Potting tests*
  PP material adsorbs exclusively the organic solvent that is used in the potting material (acetone). This affects a changed kinetic of the potting materials hardening process (Figure 29). The material does not stay flexible, but becomes hard and cracky. A changing in the composition of potting material is generally possible but takes a lot of time because a lot of design work and many trials needs to be processed for this.

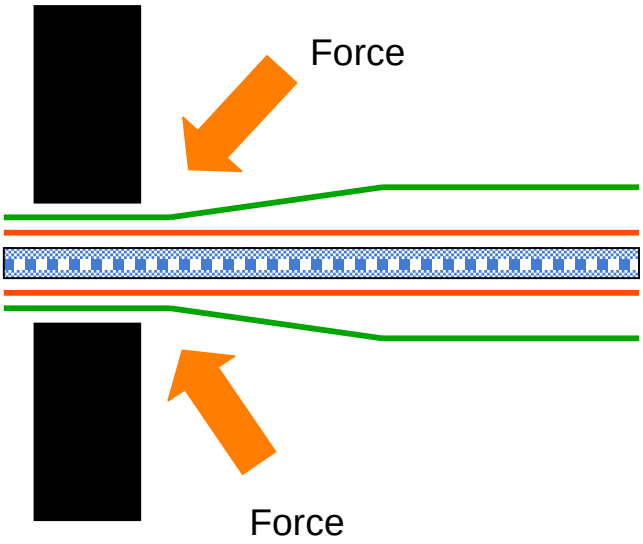

Figure 29 –Layout of the potting

Potting is better possible with the PA membrane, but this material adsorps the whole potting material, what is not critical.

3.2 Electrospun nanofibers for filtration applications

Electrospun nanofibers were produced with the apparatus designed and constructed in TTX. The most suitable condition for the production of nanofibers with the monosyringe configuration are listen below:

- Flow rate: 5 ml/min
- Polymer concentration: 18%
- Distance between the electrode:9 cm
- Voltage in the range 25 kV

SEM analysis shows that in the selected condition a dense nanoweb is produced with a small amount of defects, such as coagulum induced by the agglomeration of polymer in the web and/or dissolved area induced by the dropping of solvent induced by the deposition of material in the same area (Figure 30).

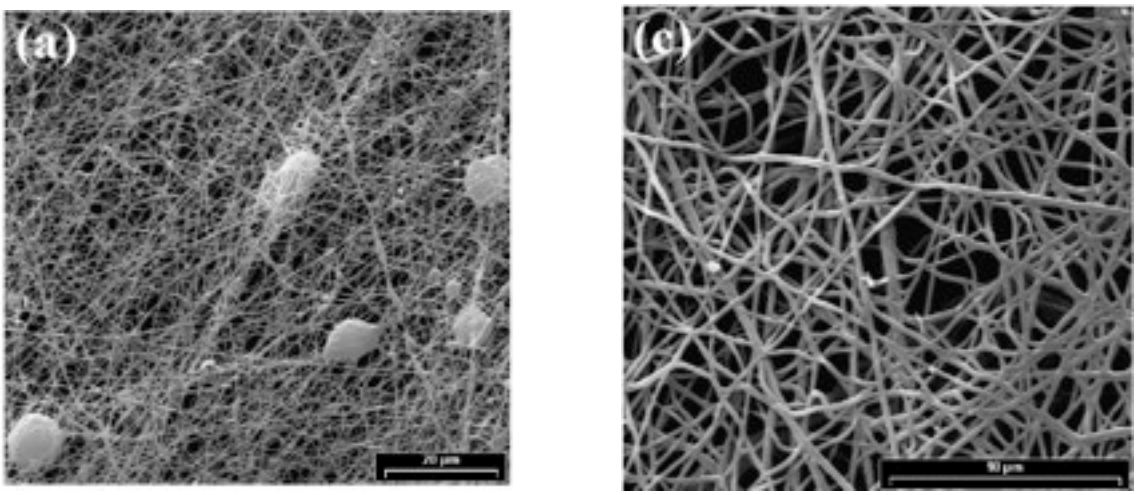

Figure 30 - SEM picture of the nanoweb produced in the optimised conditions at two different magnification.

The pictures show also that a quite dense nanoweb is produced.
The apparatus is able to produce nanofiber with a mean diameter of around 250 nm with a narrow distribution around this value (Figure 31).

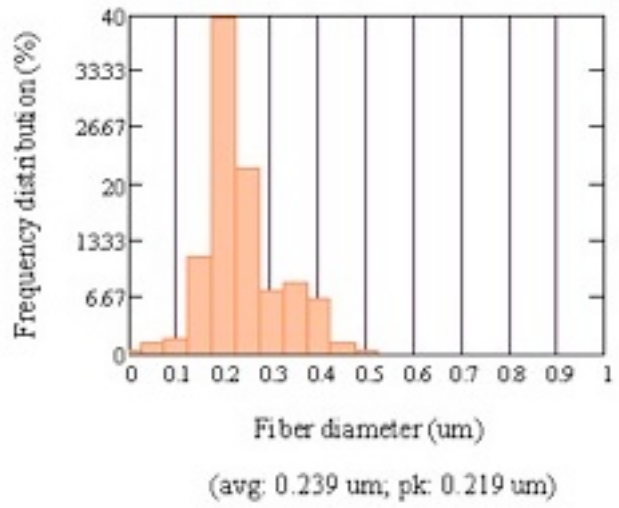

Figure 31 – Distribution of the nanofiber diameter

To ensure a large production of the nanoweb the design of a multisyringe systems was investigated by applying the process parameters optimised with the monosyringe one.
The following configurations were investigated:

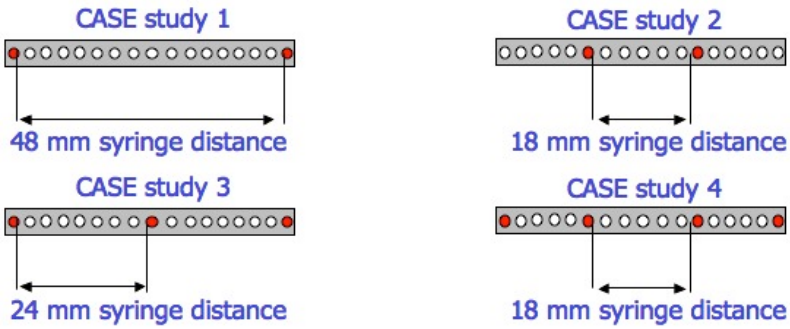

The most suitable system is the three syringes ones (distance between the nozzles = 24 mm) since this configuration ensures the maximum performances in terms area covered by the nanoweb and its density and quality. In fact, SEM analyses performed on the different configuration showed that by

increasing the number of syringe increase the density of the nanoweb (Figure 32), even if when the distance between the syringes became too small a strong interaction between the Taylor cones is achieved. This overlapping induces a too strong dissolution of the nanoweb promoted by the solvent dropping.

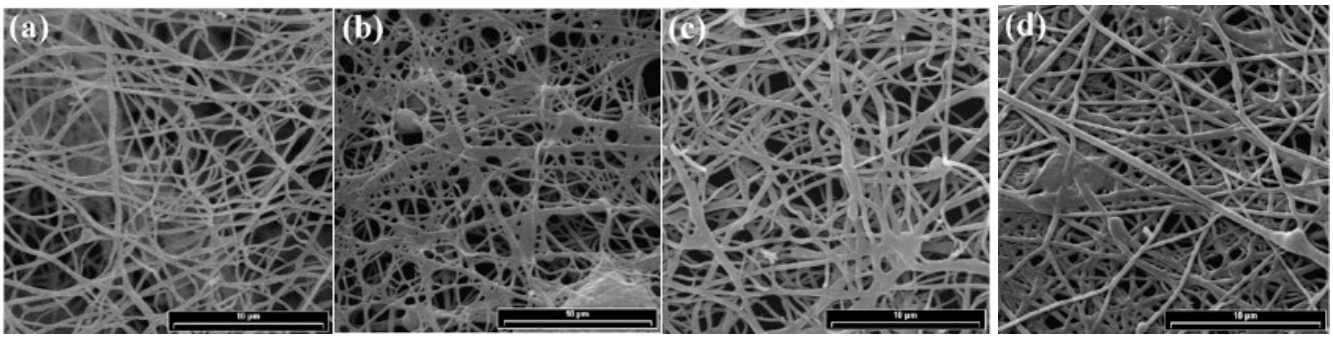

Figure 32 - SEM micrografies related to the different multisyringe systems studied at TTX: a) two syringe system (distance between syringes 48 mm); b) two syringe system (distance between syringes 18 mm); c) three syringe system (distance among syringes 24 mm); d) four syringe system (distance among syringes 18 mm).

The most suitable system is the three syringes ones. The diameter of the nanofiber produced with the studied systems show more o less the same value recorded for the monosyringe one.
The optimised configuration and working conditions were applied to coat the nylon 6 nanoweb on the PP and PA membranes (pore size 25 μm for both membranes) produced by TTX.
SEM analyses performed on the coated non woven membranes showed that the nanoweb is coated on textile surface even if with the static configuration (1st configuration) is not able to ensure a homogeneous distribution (Figure 33, Figure 34) for both substrates.

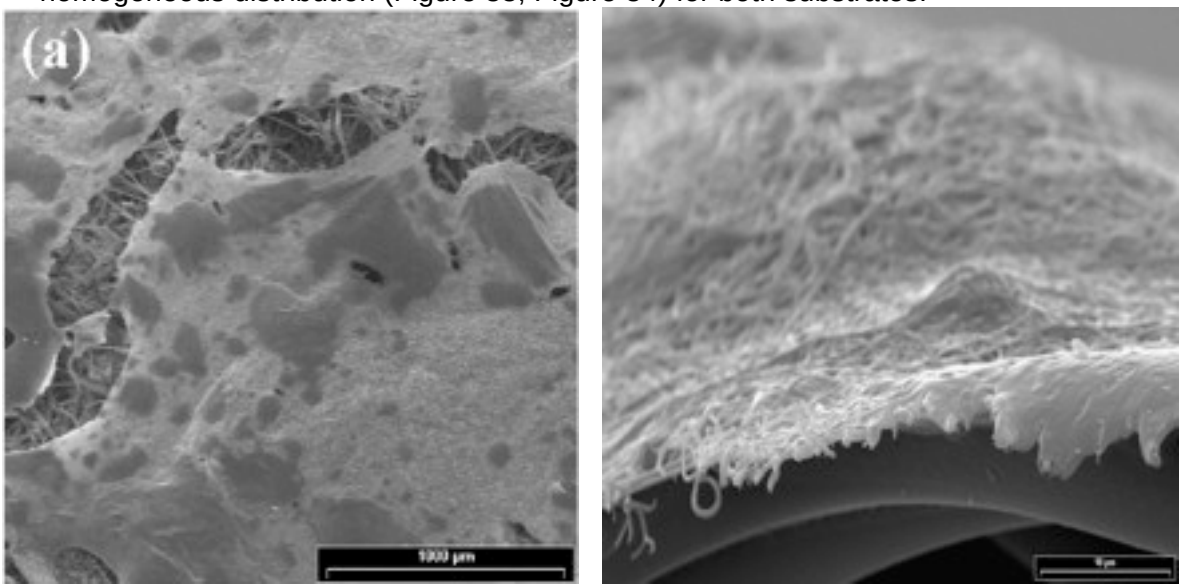

Figure 33 - SEM picture of the PA 25 μm textile membrane coated with nylon 6 nanoweb

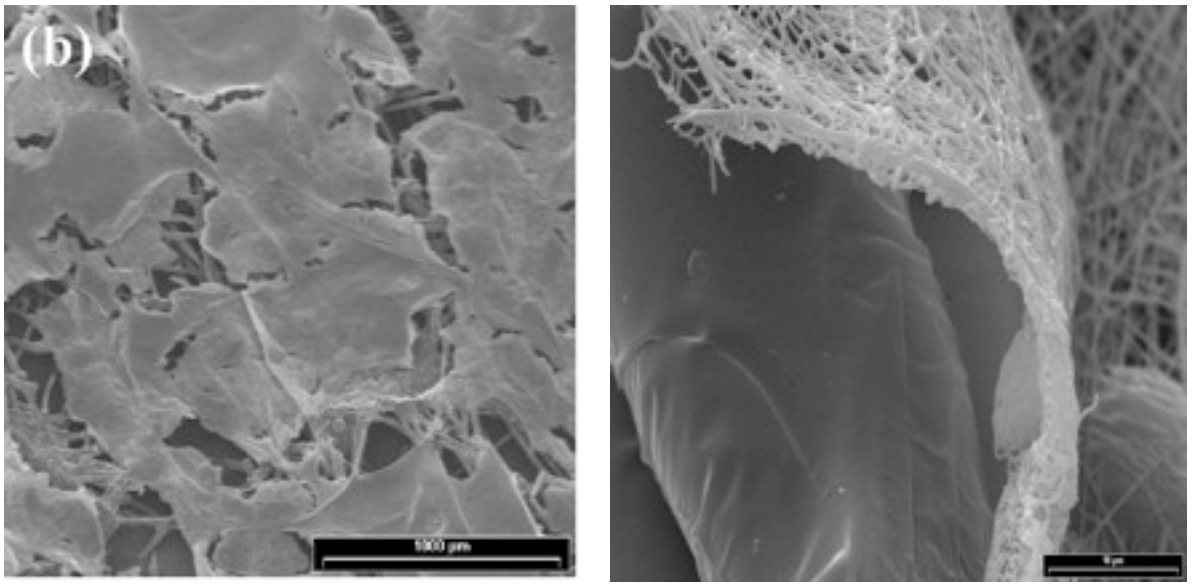

Figure 34 - SEM picture of the PP 25 μm textile membrane coated with nylon 6 nanoweb

It's interesting to note that since the PP is an apolar medium whilst PA is a polar one, the nylon 6 nanoweb have a less chemical affinity with PP; in fact the polar groups of PA can interact with the nylon 6 polymer by means of low energy interaction (Van der Walls forces or polar interactions), even if the roughness of the substrate ensures a quite good adhesion of the nanoweb to the nonwoven surface.
The nonwoven membranes coated with the nanofibers were then characterised by means of:

- Chemical Resistance to acid (HNO3, 1 M at pH < 2); to alkali (NaOH, 1 M at pH > 12); to chloride (NaOCl, 1000 ppm) and to hydrogen peroxide (H2O2, 500 ppm);
- Pore Size Analyses;

by applying the same methods used for the characterisation of the commercial and newly realised non woven membranes.
Concerning the chemical resistance tests, the results showed that the tensile strength and resistance does not depend on the nanoweb, but only the bulk affects these parameters. Only a slight increase in the degradation induced by acid is recorded since nylon 6 was dissolved is dissolved in acid environment.
An opposite trend is achieved concerning the pore size distribution: the deposition of the nanoweb onto the nonwoven structure is able to reduce the dimension of the pores.
The distribution of the pore size for the PA non woven membrane coated with the nylon 6 nanoweb (Table 12), evaluated in three different area showed that a significant reduction on the diameter at maximum pore distribution is recorded after nanoweb coating.

Table 12 - Pore size of the PA non woven membrane coated with the nylon 6 nanoweb compared to the PA non woven membrane without coating.

Sample ID	Mean Pore Size [μm]	Pore Size at maximum distribution [μm]
PA_25μm	23.1887	29.097
PA_NY6	26.8323 29.8059 *6.7707*	*0.6076* 32.5486 *1.9786*

The mean diameter value was affected only in one measurement; this outcome confirms that the coating is not homogeneously distributed on the surface.
The same results were also recorded for the PP membrane (Table 13).

Table 13 - Pore size of the PP non woven membrane coated with the nylon 6 nanoweb compared to the PP non woven membrane without coating

Sample ID	Mean Pore Size [μm]	Pore Size at maximum distribution [μm]
PP_25μm	25.4731	28.7561
PP_NY6	23.6008	*3.2553*
	22.2705	36.4622
	20.5793	*4.2503*

In order to optimise the deposition of the nanofiber onto the non woven membrane surface and the homogeneity of the nanocoating, the production of nanofibers with the 2nd configuration of the electrospinning prototype is started.
In the condition optimised with the prototype set with a plate collector (1st configuration), nanofibers were produced with the new design (drum collector):

- •Flow rate: 5 ml/min
- •Polymer concentration: 18%wt.
- •Distance between the electrode :9 cm
- •Voltage in the range 25 kV
- Three syringes

SEM analyses (Figure 35) showed that the nanowebs produced by means of the new apparatus are denser and with less defects than the ones produced with the first configuration.

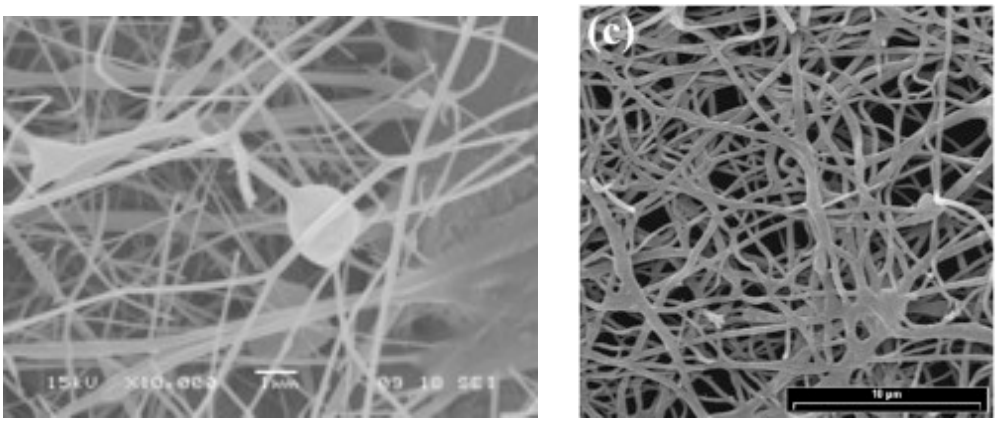

Figure 35 - SEM picture of the nanoweb produced with the drum collector compared to the nanoweb produced with the first configuration.

In order to improve the efficiency of the system, the flow rate was reduced to decrease the amount of nylon 6 and solvent required to produce the nanoweb. The following flow rate values were investigated: 5 ml/min (Sample ID: NY6_DRUM_5.0), 2.5 ml/min (Sample ID: NY6_DRUM_2.5), 1.5 ml/min (Sample ID: NY6_DRUM1.5), 1 ml/min (Sample ID: NY6_DRUM_1.0), 0.75 ml/min (Sample ID: NY6_DRUM_0.75), 0.5 ml/min (Sample ID: NY6_DRUM_0.5), 0.25 ml/min (Sample ID: NY6_DRUM_0.25) ,0.1 ml/min (Sample ID: NY6_DRUM_0.1).
It was found that by decreasing the flux, the homogeneity of the nanoweb is not affected whilst an increase on the density is recorded by decreasing the flow rate (Figure 36).

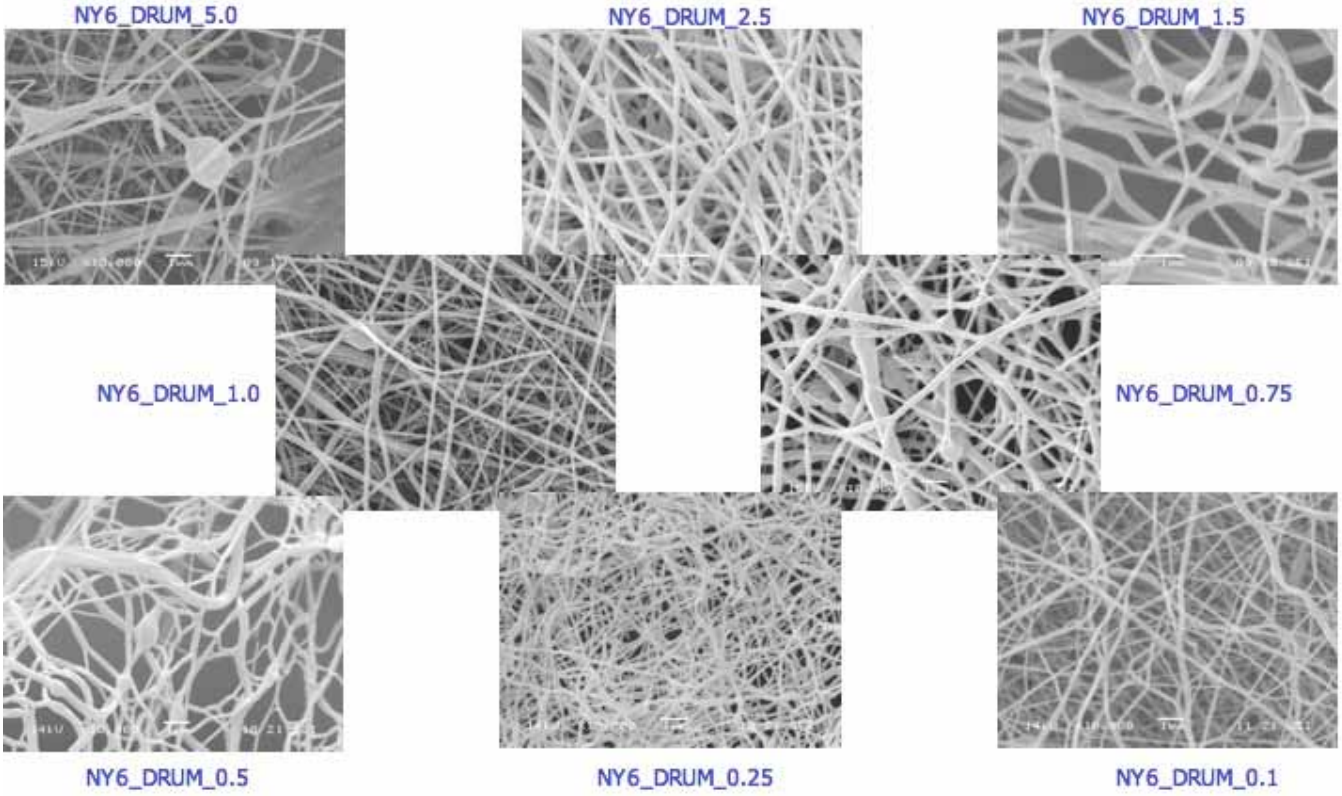

Figure 36 - SEM picture of nanowebs produced at different flow rates.

The most suitable conditions (Table 14) were applied for the deposition of the nanofibers onto nonwoven membranes both commercial (Freudenberg FF2007) and newly realised by TTX.

Table 14 – Optimised condition for the production of nanofiber onto nonwovens membranes

Parameters	Optimum value
Polymer concentration [%wt.]	18
Distance electrodes [cm]	9
Voltage [kV]	30
Flow rate [ml/min]	0.25
Syringe distance [mm]	24
Drum Speed [Hz]	35

The main benefits induced by the application of the nanoweb onto Polypropylene nonwoven membranes were the reduction of the roughness and the reduction of the pore size that show values comparable with the ones obtained with the control membrane (A3 PVDF polymeric membrane).
SEM analyses concerning the nanoweb show that the nanoweb is homogeneously deposited all over the nonwoven support (Figure 37).

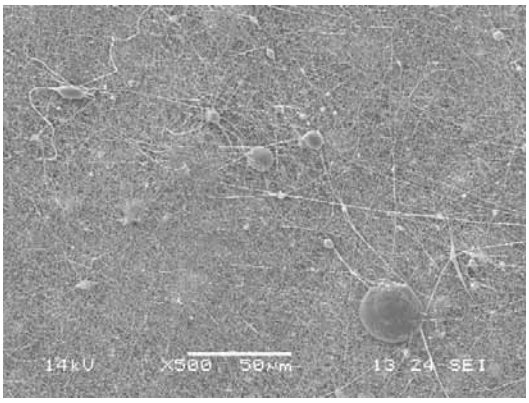

(a)

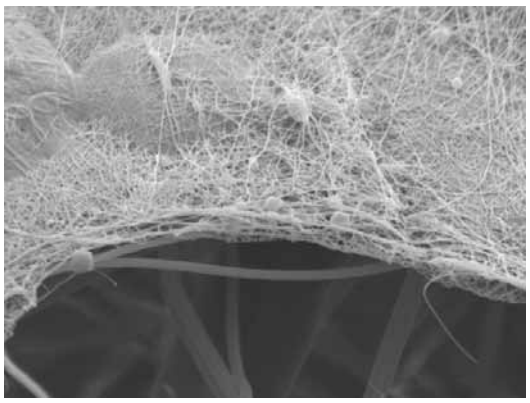

(b)

Figure 37 – SEM analysis of the NY6 nanoweb deposited onto nonwoven membranes by means of electrospinning in the optimised conditions. (a) surface micrography (b) width micrography.

The analyses showed that the diameter of the nanofiber is around 200 – 250 nm, as previously recorded. Furthermore, the width of the nanoweb is computed and it's around 12 – 18 µm.
In order to verify the effects of the nanoweb on the mechanical performance were evaluated by means of Standard Test (ASTM D638). The results showed that after the deposition of the nanofibers a slight increase in the tensile strength and in the elongation was recorded: 0.1 MPa and 5% respectively.

Roughness measurements
The topographic measurements showed that the nanoweb is able to significantly reduce the roughness of the treated nonwoven membranes (Table 15).

Table 15 – Roughness measurements for the nonwoven membranes coated with nanofibers compared with the untreated ones.

Sample ID	Side	Sa - Mean Value [µm]	Sq - RMS [µm]
A3_control	A	1.50	1.95
	B	5.73	6.10
PP_7µm	-	8.50	10.1
PP_7µm_nano	-	1.70	2.05
FF2007	-	6.13	8.10
FF2007_nano	-	1.16	1.70

In fact, the smaller diameter for the nanofiber allows to reducing the empty/volume ratio with an increase of the smoothness of the surface.

Capillary Flow Porometry
The trend is confirmed also by the capillary flow porometry: the high density of the nanoweb induces a decrease of the dimension of the holes that increase the cut-off with respect to the untreated ones.

Table 16 – Pore size measurments for the nanoweb coated membranes compared to the untreated ones

Sample ID	Mean Diameter [µm]	SD [µm]
A3_control	0.29	0.14
PP_7µm	5.95	4.97
PP_7µm_nano	0.97	1.08
FF2007	10.90	0.98
FF2007_nano	0.71	0.59

The promising results achieved with the nanoweb coated membranes show that the nanofiber could represent a good option in order to overcome two of the major limits of the nonwoven membranes for MBR application, such as Pore Size and Roughness.

Technical tests on the nanoweb coated membranes was then performed in order to verify their efficiency in terms of adaptability in MBR plants and water filtration performances, according to procedures defined by TUB.

Filterability
The filterability of the filtration media with a yeast suspension (c = 0.5 g/L) was evaluated. The results were listed in Table 17.

Table 17 – Filterability of yeast suspension with different filtration media.

Sample ID	Filterability* [m^3/m^2h]
A3_control	8.4
PP_7µm	35.80
PP_7µm_nano	15.9
FF2007	28.6
FF2007_nano	9.5

*test performed under vacuum conditions

It's interesting to note that the main effect in the reduction of the pore size induced by the nanoweb is the reduction of the water flow even if the values is comparable with the one achieved with the control membrane (A3 PVDF polymeric membrane).
Biogrowth
Samples of nanoweb coated membranes were treated with a yeast suspension (c = 0.5 g/L) at around 33°C for 48 h in order to verify the amount of biofilm that cover the mambrane surface and that could affect the hydraulic performance of the filtration media. Also in this analysis, the results achieved with the textile filtration media were compared with the ones recorded with the control membrane (A3 PVDF polymeric membrane).
The amount of biofilm grown onto the investigated supports was determined by gravimetric analyses (Table 18). Since the different membranes has a different weight per square meter, the amount of biofilm is expressed as %wt. respect to the initial weight.

Table 18 – Biofilm grown onto the tested nonwoven membranes.

Sample ID	W biofilm [%wt.]
A3_control	1.16
PP_7µm	19.30
PP_7µm_nano	0.43
FF2007	39.49
FF2007_nano	5.84

It's interesting to note that the nanofibers are able to reduce significantly the biogrowth that is one of the most important problem in many membrane systems. In fact, the biofilm is responsible for the loss of flux. By applying the nanofiber a reduction in the clogging induced by the deposition of biological materials can be significantly reduced even if it seems to depend also to the structure (density and width) of the support materials.
The pore size after biofilm growth was also investigated in order to evaluate the clogging induced by the fouling.

Table 19 – Mean Pore Size of the tested nonwoven membranes after the biogrowth compared with the values for the untreated ones.

Sample ID	Pore Size [µm]	Pore Size Biofilm [µm]
A3_control	0.29	< 0.1
PP_7µm	5.95	3.05
PP_7µm_nano	0.97	0.45
FF2007	10.90	6.27
FF2007_nano	0.71	0.28

Ageing Tests

The membranes were then exposed to an ageing test in order to verify the performances of the membranes after a chemical resistance treatment simulating the cleaning process and after the biofilm formation. Treated membranes were characterised by means of gravimetric analysis (only for cleaning), SEM analysis (only for cleaning) pore size measurements, roughness measurements and contact angle measurements.

The tests concerning with the cleaning process in acid condition (pH = 2 with HCl) and in alkali condition (pH = 10 with NaOH) for 24 h, showed that no significant changes are induced by the treatments.

Gravimetric analysis showed that the nylon 6 nanofibers are resistant to alkali and acid solutions since no significant loss of weight is recorded (Figure 38).

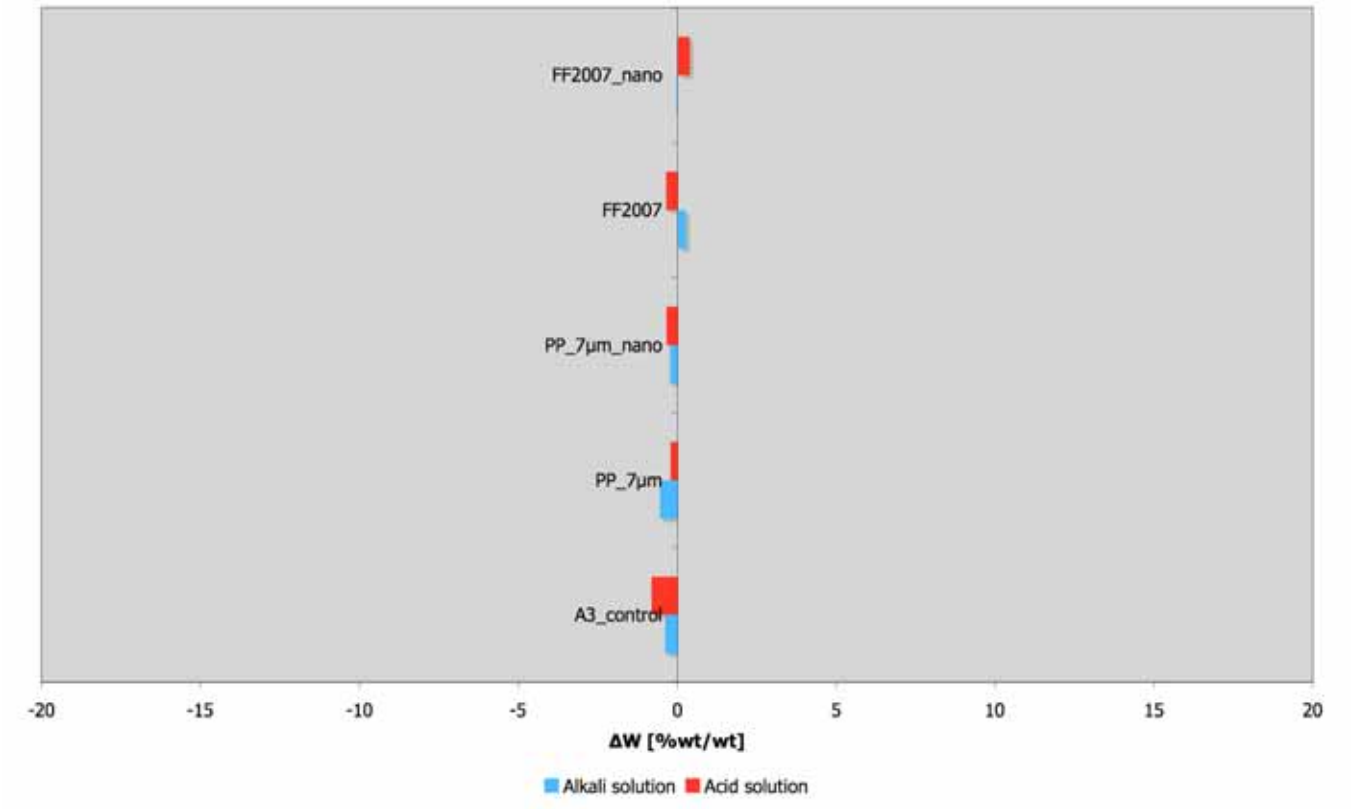

Figure 38 – Gravimetry analyses of the investigated membranes in alkali and acid solutions according to the procedure defined in collaboration with TUB.

The SEM analysis for the nanoweb coated membranes confirmed that the composite membrane is not affected by both alkali and acid solution (Figure 39).

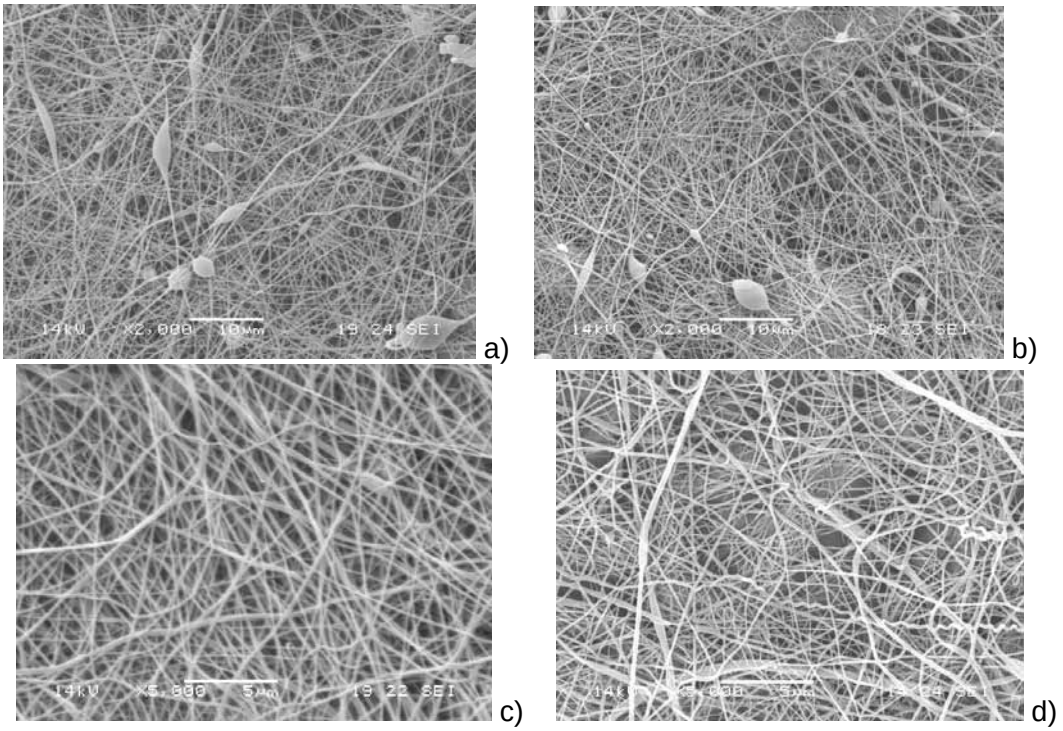

Figure 39 – SEM micrografies of the nanofiber coated membranes after the acid and alkali treatments: a) PP_7µm_nano after treatment with HCl solution; b) PP_7µm_nano after treatment with NaOH solution; c) FF2007_nano after treatment with HCl solution; d) FF2007_nano aftert treatment with NaOH solution.

The morphology of nanoweb is the same observed for the untreated nanoweb coated membranes.
Roughness measurements performed on the nanoweb coated membranes confirm that no difference in the morphology of the nanofibers is induced (Table 20).

Table 20 – Roughness measurements on on newly realised nanoweb coated membranes and on commercial membrane coated with nanoweb.

Sample ID	Side	Sa - Mean Value [µm]	Sq - RMS [µm]
PP_7µm_nano	-	1.70	2.05
PP_7µm_nano_HCl	-	1.34	1.92
PP_7µm_nano_NaOH	-	1.16	1.62
FF2007_nano	-	1.16	1.70
FF2007_nano_HCl	-	1.23	1.92
FF2007_nano_NaOH	-	1.50	2.08

On the contrary, capillary flow porometry shows that pore size is slightly affected by the treatments (Table 21), probably because of the low adhesion of the film on the supports.

Table 21 – Pore Size analyses on newly realised nanoweb coated membranes and on commercial membrane coated with nanoweb.

Sample ID	Mean Diameter [µm]	SD [µm]
PP_7µm_nano	0.97	1.08
PP_7µm_nano_HCl	1.73	1.89
PP_7µm_nano_NaOH	1.87	1.96
FF2007_nano	0.71	0.59
FF2007_nano_HCl	0.88	2.13
FF2007_nano_NaOH	1.14	2.29

Because of the interesting performances of the Nylon 6 nanoweb coated textile membranes they were coated into two different textile - Novatexx 2471 and Novatexx 2413 - supports according to their adaptability to the A3 production process. The new support was covered with nylon 6 nanofibers produced by applying the same electrospinning conditions optimised for the PP support. In fact, the nanofiber production is just slightly affected by the composition of the textile support: PET is more conductive in comparison with PP, so the electrical field is negligible modified.
The performances of the nanocomposite membrane in comparison with the A3 control are listed in Table 22.

Table 22 – Chemical and Physical Characteristic of the nanocomposite membrane in comparison with the PVDF membranes.

Type	Novatexx 2471 nano	Novatexx 2431 nano	A3 control
Material	PP (support) Nylon 6 (nanofiber)	PET (support) Nylon 6 (nanofiber)	PVDF/PET
Pore Size	0.71 µm	0.85 µm	0.29 µm
Roughness	1.16 µm	1.47 µm	1.50 µm
Tickness	0.20 mm	0.21 mm	0.20 mm
Tensile strength	15 MPa	17 MPa	21 MPa
Eloingation	25%	25%	25%
Biofilm growth	0.9%wt.	1.0%	0.6%
Alkali resistance (pH = 10)	Y	Y	Y
Acid resistance (pH = 2)	Y	Y	Y

A study concerning the scale-up of the production processes of the nanocomposite membrane and its costs were assessed. The main issue related with this kind of membrane is the scale-up of the electrospinning process from lab-scale to industrial-scale. However, industrial electrospinning equipments are commercially available! TTX contacted one of the most important producer (ELMARCO, Czech Republic) and on the basis of the performance and productivity of its equipment it was possible to make an estimation of the production costs for the nylon 6 nanocomposite membranes (Table 23).

Table 23 – Estimation of the production costs for the nanocomposite membranes

Expenditure	Cost	Cost (€/m^2)
Material	-	***0.024***
Nylon 6	2.00 €/kg (UFI)	0.007
Formic Acid	0.65 €/kg (BASF)	0.017
Support	3.87 €/m^2	***3.870***
Investment *	600,000 € (ELMARCO)	***1.151***
Energy	0.13 €/kWh	***0.044***
TOTAL	-	***5.132***

* 5 year depreciation

The production costs of the nanocomposite membrane are 60% higher then the target value reported in the DoW, but we have to highlight that 75% of the total cost is due to the nonwoven support, we are confident that we could significantly decrease the cost of the nanocomposite membrane by selecting nonwoven support with lower prices since smooth surface of the surface are not required as per casting production of conventional microfiltration membranes. In any case, by applying the membranes set-up within AMEDEUS project, around 9.00 €/m^2 can be saved considering that the cost of commercial PVDF membrane is 14.00 €/m^2 (cost reduction is 63%).

Adequacy of the nanoweb coated membrane in MBR module

The tests performed by A3 on Polypropylene membranes (section 3.1.8) showed that the main parameter that PP membrane was better than PA membrane concerning the cushion process even if the large pore size and the adsorption of the glue solvent were the main parameters limiting the adequacy of PP membrane in MBR module.
The pore size is efficiently reduced by applying the nanofiber onto nonwoven membrane, as demonstrated above, whilst to modify the potting behaviour of the PP (Fredeberg membrane was selected as a model for Polypropylene membranes in agreement with A3), the nanoweb coated membranes were treated with a commercial fluorocarbon resin (Rucostar, Rudolf Chimie). In fact, fluorinated compounds are able to decrease the superficial tension of textile and nonwoven surface[xxvi]. The adsorption of liquids from a substrate is controlled by this parameter. A commercial product was applied in order to generate a frame all around the membrane sheet (Figure 40) and it was applied by means of a padding machine operating at different drum pressures.

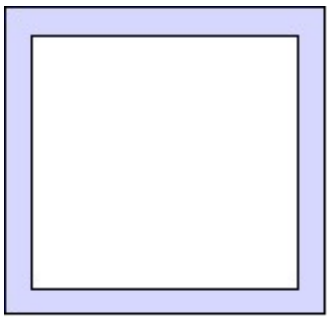

Figure 40 – Layout of the application of fluorocarbon onto textile surface

Squeezing pressure of 6 bar was found as the optimal pressure enable to reduce efficiently the adsorption of acetone (solvent of the glue), as demonstrated by measuring the height of the acetone absorbed by the membrane after exposure to the solvent for 20 seconds. A schema of the used procedure is represented in Figure 41.

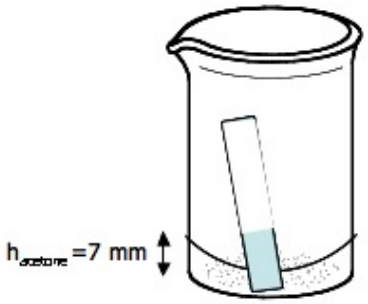

Figure 41 – Schema of the procedure used for measuring the adsorption of acetone by the nonwoven membrane coated with a flurorocarbon.

The height values related with the adsorption of acetone are listed in Table 24.

Table 24 – Adsorption of acetone after fluorinated coating

Sample ID	h [mm]	exposition time [s]	Δh [%]
FF2007	47	20	-
FF2007_Fluoro_2bar	41	20	-13%
FF2007_Fluoro_4bar	34	20	-28%
FF2007_Fluoro_6bar	26	20	-45%

Samples of fluorinated and non–fluorinated nanoweb coated membranes were tested at A3 in order to validate the membrane with the production process applied by the company. Concerning the cushion process the following conditions were applied:

- Temperature: 160 °C
- Heating time: 30 – 40 s
- Embossing time: 30 s

The main problems related with the textile material both untreated or treated with the fluorocarbon are that on the one hand longer heating time and a higher temperature than during the tests are necessary but on the other hand the membrane already melts during the conditions of the tests. Because of the short heating time and the “low” heating temperature the pores of the currently used base are not heat-sealed

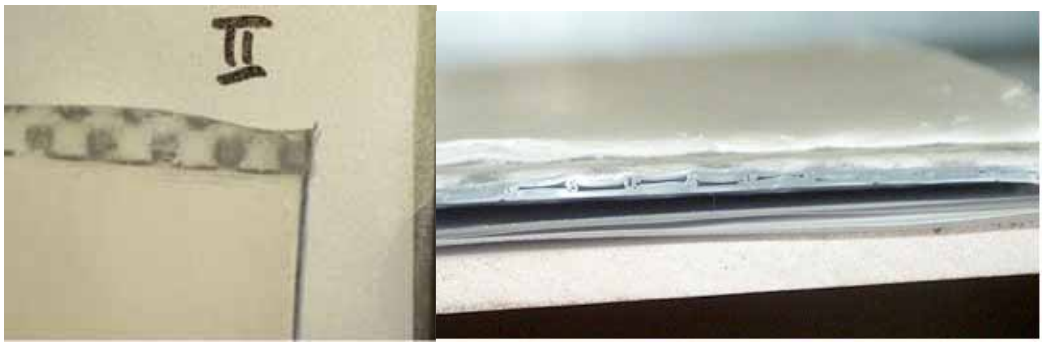

Figure 42 – Pictures of the surface and section of the nanoweb coated membrane sealed to the support with the A3 procedure. No differences were found on the membrane treated with fluorocarbon.

Furthermore, when Potting Tests were carried out on the investigated substrates showed that after priming a 10 mm wide stripe the membrane surface lifts (ca. 20 mm) from the base (Figure 43).

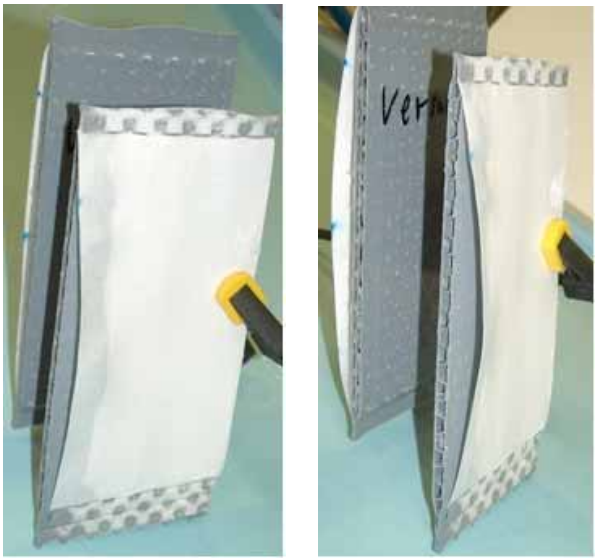

Figure 43 – Detachment of the membrane after priming

On the contrary, the membrane material which is coated with nanoweb and fluorocarbon is not soaked with the grouting and the tensile strength is very low and the module rips open whilst the Freudberg membrane coated with nanoweb is soaked and showed a higher tensile strength than the fluorinated one.


a)
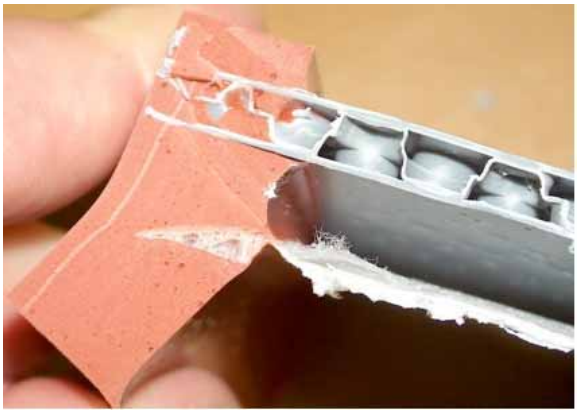
b)

Figure 44 – Sealing performances of the nanoweb coated Freudeberg membrane treated with fluorocarbon (a) and of the nanoweb coated Freudeberg membrane (b).

The lower tensile strength of the module with the nanoweb and fluorocarbon coated membrane is very critical. It will be expected, that the light interconnection between the membrane and the grouting isn't strong enough to resist the resulting forces. This problem doesn't exist by using the Freudenberg membrane coated with nanoweb.
In any case because of the high heating time required to heat-seal the pores of the base and the melting of the membrane surface and mechanical the sensitivity of the membrane material, the Freudenberg F2007 membrane is not a suitable membrane for the currently production procedure applied in A3.
To overcome the limits of the adaptability of the Freudenberg membrane in the A3 production line minor modifications may be undertaken to make it compatible with textile fabrics (i.e. change of support material) and the selection of a different textile membranes (i.e. Polyester membranes) can be assessed.

The first solution that has been exploited was the replacement of the Polypropylene support with a Polyester membrane, Novatexx 2413N provided by Freudenberg and selected in collaboration with A3.

The adaptability of the new nanocomposite membrane is quite good: the membrane backing material does not lift, even if its rising is high and it could cause some problem in the gluing of the membranes. However, the tensile strength is comparable with conventional membranes.
The optimal condition for the potting of the membranes are listed below:

- heating time between 25 and 30 seconds
- heating temperature 220 °C.

In these conditions, the backing material is not melting and the connection with the base plate is strong.

Moreover, a new support (Novatexx 2471) has been selected in collaboration with Freudenberg since it could be a suitable option for the application of Polypropylene for the production of filtration modules because of its high tensile properties. Some tests have been performed and they showed that this backing materials can be easily processed then the previous ones.

Filterability of plasma treated and nanocoated membranes

The results for the critical flux measurement can be seen in Table 25. As it can be seen a nanocoating generally higher critical fluxes that then the conventional textile.
It could be observed that the virgine Freudenberg textile blocked quickly and was brownly discoloured. The nanocoating obviously leads to smaller pore sizes which can not easily be encountered by fine particles. There no change of colour was noticed after the experiment.

Table 25 – Critical flux for Freudenberg FF2007 nonwoven with and without nanocoated NY6

Sample ID	J crit
FF2007	25
FF2007_nano	75

A second set of tests were conducted with a different carrier Material from Freudenberg (Novatex 2413N). These were conducted due to the promising and stable composition of this material. If the separation takes place on top or within the nanocoating the type of support material should not cause any difference in filtration performance. Nevertheless for textiles and very thin nanocoatings the filtration might still take place within the carrier. Therefore this second support was tested and similar performances where recorded.

For the production of small scale filtration modules for TBR (textile bioreactor) pilot tests, the virgin Freudenberg NOVA2413 and NOVA2413_nano were used due to the better adequacy to the A3 production.

Permeate quality

Table 26 shows the permeate quality in terms of colony forming units (CFU) for unfiltered sludge und sludge filtered with different textiles. Already the filtration with the relatively rough Novatex textile alone shows a reduction of more than 90% in CFU. The addition of the flocculant does not increase this significantly. Nevertheless the nanocoating further reduces the CFU for another 10%.
Common UF or MF membranes are close for bacteria unless some defects in membrane material occur. This can not be reached by the produced nanotextiles, even if further development could allow to reduce this parameter by increasing nanoweb adhesion onto the selected substrate.

Table 26 – Permeate quality for Freudenberg nanocoated Novatex

Sample ID	CFU/ml permeate
Unfiltered sludge	>50,000
Filtered sludge (25µm)	24,800
NOVA2413_nano	4000

3.3 Pilot-scale Test with TBR

According to the promising results achieved with the nanocomposite membrane it was decide to construct three different textile modules: one realised with the NOVA2413_nano membrane, one realised with the NOVA2471_nano membrane and the latter realised just using the Novatexx 2431N membrane. The characteristics of the textile modules are listed in Table 27.

Table 27 - Characteristic of the Textile MBR modules

Composite Textile Bioreactor	
Number of plate per unit	8
Membrane per plate	2
Membrane dimension	0.10 x 0.15 m^2
Total filtration area	0.24 m^2

Filtration performance

Figure 45 shows the filtration performance of the Novatex and nylon 6 nanocoated Novatex module in the TBR. Three different aeration intensities were tested as it is assumed that a lower aeration might be beneficial for the operation of TBRs[xxvii ;xxviii]Generally the filtration with the nanocoated textile Novatex_nano seems to be more stable and sustainable than the filtration with the coarse nonwoven Novatex. The smaller pores are probably not easily penetrated by sludge flocs and seem to be less susceptible for fouling. The addition of the synthetic WWT causes a jump in the TMP curve and a decline in the flux. The feed was added twice a day in a high concentration directly into the filtration tank. The negative effect might thus be due to a stress situation of the microorganisms due to the high organic load and a release of SMP or to fouling mechanisms in or on the membranes by the WWT components. For further trials the feed should be dosed continuously into a upstream compartment in order to avoid peak loads and direct contact of WWT constituents with the membrane. For both textile modules the best performance was found for the medium aeration of 1.1m³/h. For the lower aeration the cake is obviously not removed effectively, at a aeration of 5m³/h the shear stress is probably to high, leading to smaller sludge flocs and classification in terms of particle size on the textile surface. It must be noted that the very high permeability shown in the critical flux tests (Table 26) in the test cell trials could not be achieved in the TBR trials. This must be due to differences in hydrodynamics. Although a similar aeration was used (in terms of superficial air velocity) in the test cell trials, the circulation velocity was surely higher in the test cell (0.2m/s). Due to the low water level in the lab-scale TBR (0.7-0.8m) the sludge velocities due to the airlift loop reactor are quite low compared to large scale MBRs. Further large scale tests would be necessary to evaluate this.

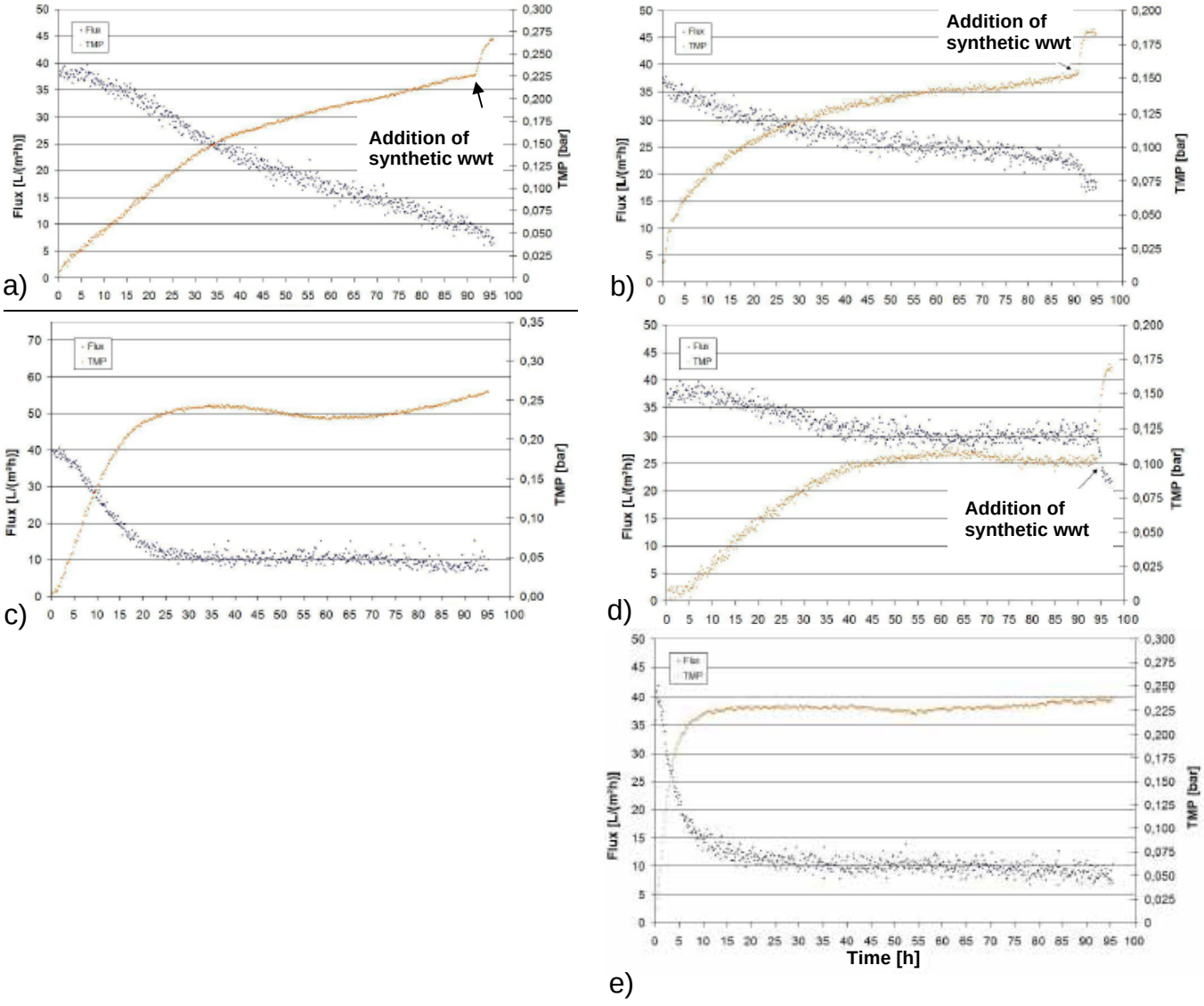

Figure 45 – a) Performance of the Novatex module b) performance of the nanocoated Novatex module, 0.34 m³/h aeration c) Performance of the Novatex module d) performance of the nanocoated Novatex module, 1.1m³/h aeration e) performance of the nanocoated Novatex module, 5 m³/h aeration

Permeate quality in the TBR

The permeate quality in terms of CFU for different days of operation for the two tested modules are shown in Table 35. The results are shown for the experiments shown in Figure 45. The number of bacteria found is much lower than for the test cell trials (Table 26). This is in accordance with the lower permeability – which indicates a stronger fouling layer functioning as a secondary filter layer. . The number of bacteria is thus strongly reduced by the textile filtration media, but does still not meet the requirements of the European bathing water directive.

Table 28 – Permeate quality for Freudenberg nanocoated Novatex_nano in the TBR

Sample ID	Day	CFU/ml permeate
NOVA_nano	1	730
	3	620
	5	460

Recovery after cleaning

After each trial the textile module was cleaned physically (rinsing with water for 20 min) and chemically (by soaking in 1500ppm chloring solution). The effect of the cleaning was evaluated by determining the recovery factor Y:

$$Y = \frac{permeability\ after\ cleaning}{initial\ permeability\ of\ the\ \mathrm{module}}$$

The recovery factors for the cleaning of the nylon 6 nanocoated on Novatex supports are shown in Table 29. .

The recovery after the physical cleaning is below 20% for the nanocoated textile; so the chemical cleaning step is essential to have a sufficient cleaning. The fouling seems to be more persistent.

Table 29 – Cleaning efficiency for Freudenberg nanocoated Novatex

Cleaning step	Nanocoated Novatex
1st physical cleaning	0.11
1st chemical cleaning	0.83
2nd physical cleaning	0.18
2nd chemical cleaning	0.66

4 Conclusions

Results achieved during the first year of the project showed that the stationary flux of the textile filters is in the range of the microporous polymeric membranes and they have a higher initial flow and a higher permeability then the reference. During long term filtration some textiles clogged very quickly and showed a deficient permeate quality. Crucial points to be solved are the pore size (distribution) and the roughness of the material.
From the chemical point of view, textile seems to ensure the same performances in comparison with the conventional membranes and the polypropylene nonwoven seems to ensure the best resistance.
The characterisation of both newly realised membranes and commercial membranes showed that the textile membranes have larger pore sizes then the conventional ones with a large pore distribution, even if by modifying production conditions it is possible to control this parameter.
Since a random distribution of fibres generates the webs, higher roughness was recorded for textile filters even if the tests realised on newly realised membranes indicate that it's possible to reduce it, by controlling the production working parameters.
The optimisation on the production of the nonwoven membrane in term of thickness and density of the polymer can also increase the possibility of the application of these textiles as replacement for membranes in MBR plants.
In order to easily solve the limits of the textile filtration media electrospinning seems to be a promising option.
The coating of nanoweb allows reducing some critical points, such as porosity and roughness mainly responsible for the low filtration performances. During long term operation on the TBR, the nanocoated material showed better results than the coarse nonwoven delivered by Freudenberg. It was possible to operate the nanocoated module at a flux of 30L/(m²h) for 3d. The test cell trials indicate that fluxes up to 150 L/(m²h) might be possible. Further studies are necessary here. Investigations of the number of bacteria in the permeate showed that these decrease with time due to the build up of the filter cake. The high standard of MBR effluent was not reached within the 5 days operation time.
Further research is necessary in the field of permeability recovery by physical/chemical cleaning, as fouling and cleaning phenomena might strongly differ from conventional microporous membranes.

5 References

[i] Handbook of Membrane technology, M. C. Porter, Noyes Publications – Westwood New Jersey (USA), 1990.

[ii] Zhi-Guo, M., Y. Feng-lin, and Z. Xing-wen, *MBR focus: do nonwovens offer a cheaper option?* Filtration + Separation, 2005. 42(4): p. 28-30.
[iii] J.A. Destephen and K. Choi, Modelling of filtration processes of fibrous filter media, Sep. Tech. 6 (1996) 55-67.

[iv] G.T. Seo, B.H. Moon, T.S. Lee, T.J. Lim and I.S. Kim, Non-woven fabric filter separation activated sludge reactor for domestic watewater reclamation, Wat. Sci, Technol., 47 (2002) 133-138.

[v] Kiso, Y., Y.-J. Jung, T. Ichinari, M. Park, T. Kitao, K. Nishimura, and K.-S. Min, *Wastwater treatment performance of a filtration bio-reactor equipped with a mesh as a filter material.* Wat. Res., 2000. 34: p. 4143-4150.
[vi] Kiso, Y., Y.-J. Jung, M.-S. Park, W. Wang, M. Shimase, T. Yamada, and K.-S. Min, *Coupling of sequencing batch reactor and mesh filtration: Operational parameters and wastewater treatment performance.* Wat. Res., 2005. 39: p. 4887-4898.
[vii] Chang, W.-K., S.-H. Chuang, A.Y.-J. Hu, and M.-C. Chang. *Nonwoven fabrics as solid-liquid separation media in membrane bioreactor*. *Filtech* 2005. Wiesbaden.

[viii] Chang, M.-C., R.-Y. Horng, H. Shao, and Y.-J. Hu, *Performance and filtration characteristics of non-woven membranes used in a submerged membrane bioreactor for synthetic wastewater treatment.* Desalination, 2006. 191(1-3): p. 8-15.
[ix] A.L. Lim, Renbi Bai; Membrane fouling and cleaning in microfiltration of activated sludge wastewater; Journal of Membrane Science 216 (2003) 279-290

[x] C O M P A C T U L T R A F I L T R A T I O N M E M B R A N E, X-FLOW Database

[xi] Rosenberger, S., A. Drews, and M. Kraume, Comparison of Microfiltration Behaviour of Activated Sludge and Model Suspensions in a Novel Membrane Test Cell. Chem. Ing. Tech., 2001. 73(6): p. 597.

[xii] Dubois M., Gilles K., Hamilton J., Rebers P. and Smith F.(1956). Calorimetric method for determination of sugars and related substances. Anal.Chem., 28(3), 350-357.

[xiii] Frolund B., Palmgren R., Keiding K. and Nielsen P.H. (1996). Extraction of extracellular polymers from activated sludge using a cation exchanger resin. Wat. Res., 30(1749-1758).

[xiv] Grafe, T., Graham, K., “Polymeric Nanofibers and Nanofiber Webs: ANew Class Of Nonwovens,” International Nonwovens Journal, Vol. 12, No. 1, 2003, 51-55

[xv] Gibson, P., Schreuder-Gibson, H., “Patterned Electrospray Fiber Structures,” International Nonwovens Journal, Vo. 13, No. 2, 2004, 34-41.

[xvi] Graham, K., Gogins, M., Schreuder-Gibson, H., “Incorporation of Electrospun Nanofibers Into Functional Structures,” International Nonwovens Journal , Vol. 13, No. 2, 2004, 21-27

[xvii] Tsai, P., Chen, W., Roth, J., “Investigation of the Fiber, Bulk, and Surface Properties of Meltblown and Electrospun Polymeric Fabrics,” International Nonwovens Journal , Vol. 13, No. 3), 2004, 17-23.

[xviii] Kyong Su Rho, Lim Jeong, Gene Lee, Byoung-Moo Seo, Yoon Jeong Park, Seong-Doo Hong, Sangho Roh, Jae Jin Cho, Won Ho Park and Byung-Moo Min, „ Electrospinning of collagen nanofibers: Effects on the behavior of normal human keratinocytes and early-stage wound healing“, Biomaterials, Volume 38, Issue 2, 30 March 2006, Pages 140-144.

[xix] Il Keun Kwon, Satoru Kidoaki and Takehisa Matsuda,“ Electrospun nano- to microfiber fabrics made of biodegradable copolyesters: structural characteristics, mechanical properties and cell adhesion potential“, Biomaterials, Volume 26, Issue 18, June 2005, Pages 3929-3939.

[xx] Eugene D. Boland, Branch D. Coleman, Catherine P. Barnes, David G. Simpson, Gary E. Wnek and Gary L. Bowlin, „ Electrospinning polydioxanone for biomedical applications“,Acta Biomaterialia, Volume 1, Issue 1, January 2005, Pages 115-123.

[xxi] Kwangsok Kim, Yen K. Luu, Charles Chang, Dufei Fang, Benjamin S. Hsiao, Benjamin Chu and Michael Hadjiargyrou,“ Incorporation and controlled release of a hydrophilic antibiotic using poly(lactide-co-glycolide)-based electrospun nanofibrous scaffolds“,Journal of Controlled Release, Volume 98, Issue 1, 23 July 2004, Pages 47-56

[xxii] G.Detall, Molecular organisation in structured PVD, J. of Mat. Science, 33 (1998) 3511 –3527

[xxiii] S.S. Madaeni, Effect of surface roughness on retention of reverse osmosis membranes, J. Poorus Mat., 11 (2004) 255 – 263.

[xxiv] Akshaya Jena and Krishna Gupta, ‘Characterization of Pore Structure of Filter Media’, Fluid/Particle Separation Journal, 14 (2002) 1.

[xxv] A. K. Jena and K. M. Gupta, ‘Pore size Distribution in Filter Materials’, Book of Papers, FILTRATION 99, International Conference, Association of the Nonwoven Fabric Industry (1999) p.24.0.

[xxvi] Babu S.V.; Srividya C.; Visser S.A.; Hewitt C.E.; Fornalik J.; Braunstein G, Compositions and surface energies of plasma-deposited multilayer fluorocarbon thin films, Surface and Coatings Technology, 96 (1997), 2, 210-222

[xxvii] Fuchs, W. ; Resch, C. ; Kernstock, M. ; Mayer, M. ; Schoeberl,P. ; Braun, R.: Influence of operational conditions on the performance of a mesh filter activated sludge process. *Water Research* 39 (2005), S. 803–810

[xxviii] Loderer, C. ; Aichberger, G. ; Fuchs, W.: Pilot plant experiences using Mesh filter modules for direct activated sludge separation. *IWA World Water Congress and Exhibition*. Wien, 2008